AEDC-TR-61-6

ARCHIVE COPY
DO NOT LOAN

a-1

DESIGN OF A LARGE, TWO-STAGE, LIGHT-GAS MODEL LAUNCHER

By
W. B. Stephenson and D. E. Anderson
VKF, ARO, Inc.

June 1961

ARNOLD ENGINEERING
DEVELOPMENT CENTER
AIR FORCE SYSTEMS COMMAND
USAF

AEDC TECHNICAL LIBRARY
5 0720 00030 9734

Additional copies of this report may be obtained from

ASTIA (TISVV)
ARLINGTON HALL STATION
ARLINGTON 12, VIRGINIA

note

Department of Defense contractors must be established for ASTIA services, or have their need-to-know certified by the cognizant military agency of their project or contract.

DESIGN OF A LARGE, TWO-STAGE, LIGHT-GAS MODEL LAUNCHER

By

W. B. Stephenson and D. E. Anderson

VKF, ARO, Inc.

June 1961

AFSC Program Area 750A, Project 8950, Task 89600
ARO Project No. 386079

Contract No. AF 40(600)-800 S/A 11(60-110)

AF - AEDC
Arnold AFB Tenn

ABSTRACT

A procedure is outlined for computing the performance of two-stage, light-gas launchers using helium as a propellant. The effects of the physical variables; geometry, piston mass, and pressures, are discussed. Design criteria are established for a large launcher which will be built for the Arnold Center (AFSC) ballistic range facility. Theoretical performance curves are included as well as experimental results obtained from two small launchers.

CONTENTS

TABLES

ILLUSTRATIONS

NOMENCLATURE

A	Cross-section area
a	Acoustic speed
$C, \tilde{M}$	Dimensionless piston mass parameters
C_v	Constant volume specific heat
d	Diameter
e	Internal energy
ℓ	Length
m	Mass
P	Pressure
s	Distance
T	Temperature
t	Time
u	Velocity
u_o	Reference launch velocity, no chambrage, infinite chamber length
V	Volume
γ	Ratio of specific heats
ρ	Density

SUBSCRIPTS

c	Chamber
F	Final state in pump tube
f	Forward face of piston
L	Launch tube
M	Projectile
o	Standard
p	Piston or pump tube
R	Rear face of piston

t, s	Partial derivatives	
1	Ahead of incident shock	normal shocks
2	Behind incident shock	
3	Behind first reflected shock	
4	Behind first shock reflected from piston face	

DIMENSIONLESS COORDINATES

$\bar{s}$ $\quad \dfrac{P_F A_L}{m_M a_F^2} s$

$\bar{t}$ $\quad \dfrac{P_F A_L}{m_M a_F} t$

$\bar{u}$ $\quad u/a_F$

$\bar{a}$ $\quad a/a_F$

$\bar{P}$ $\quad P/P_F$

P_F, a_F Initial chamber conditions, corresponding to final state in pump tube

m_M Projectile mass

INTRODUCTION

Construction was begun in 1960 at the AEDC of a 1000-ft-long, variable pressure, ballistic range to be used in developmental testing of flight vehicle models. The major advantage of the aerodynamic ballistic range lies in its capability in reproducing the environment of very high-speed flight, i. e., flight Mach numbers in excess of about 10, when dissociation of the air occurs in the vicinity of the body. Here it is necessary not only to duplicate fight Mach numbers, but also actual flight speeds, stagnation pressure, and temperature. The light-gas gun type of launcher is the only presently developed method of obtaining the required velocities in the range. Hydrogen or helium is used as the propellant after it is heated by one or more of the following methods: (a) reaction of a combustible mixture of gases within the propellant, (b) adiabatic compression with or without appreciable shock wave heating, and (c) discharge of an electric arc within the propellant. Experimentation with examples of all these systems has been conducted at AEDC. The experience of the NASA Ames Research Center, Naval Ordnance Laboratory, the Canadian Armament Research and Development Establishment, and the Air Proving Ground has been drawn upon in deciding on an initial launching system for the large range. The only system which shows reasonable promise of providing the required performance (launch velocities in excess of 20,000 ft/sec) within the available time for design and fabrication is one developed at the Ames Research Center (Ref. 1). A free-piston, shock and compression heating cycle in a two-stage configuration has yielded velocities in excess of 26,000 ft/sec for light projectiles.

The electric-arc heating principle, although having satisfactory theoretical performance, has not yet reached the stage of development for practical design primarily because of contamination of the propellant during discharge.

The use of a combustible mixture of hydrogen-oxygen-helium in a single stage does not produce high enough launch velocities, and in shock heating cycles, difficulties with pre-ignition and detonation discourage the attempt to build a large-scale launcher utilizing $H_2 - O_2$ combustion as a source of energy. The use of gunpowder - heated helium is considered the most practical driver for a piston in a large 2-stage launcher.

Manuscript released by authors May 1961.

The following light-gas launchers have been used at AEDC to obtain data upon which the large launcher design has been based: (a) a 20-mm, electric-arc heated configuration operated with a 4-megajoule, inductive storage power supply, (b) a 40-mm, H_2-O_2-He combustion-heated, single-stage launcher of Naval Ordnance Laboratory design, and (c) a 20-mm or 0.5-in. caliber, two-stage configuration using the combustion heated launcher as the first stage. This latter was operated with two lengths of 40-mm pump tube.

The two-stage configuration consists of a chamber containing the first stage propellant which drives a free piston through the pump tube. Helium or hydrogen is heated by shock waves and compression ahead of the piston, forming the second-stage propellant which drives the projectile through the launch tube. There is a paucity of information in the literature upon which a design optimization can be based. Even the effects of such fundamental physical variables as piston mass, pump tube charge pressure, pump tube dimensions, and piston velocity have not been treated except through informal communications.

It was considered essential that a systematic calculation procedure be developed which would incorporate all the known variables and would provide for the introduction of whatever empirical data were available. The fabrication of a large-scale launcher is expensive and modification is time consuming; therefore, it was considered desirable to arrive at as close to an optimum design as possible. In Ref. 2, several aspects of two-stage launcher design are considered from the theoretical point of view: multiple shock compression, piston velocity, and the effect of chamber geometry on launch velocity using helium as a propellant. There remained to be determined the effects of geometry and piston mass on structural weight and launch velocity in a complete launch system.

In arriving at a design, it was assumed that sufficient performance for the initial launcher would be such that a one-caliber long, light plastic cylinder (specific gravity 1.15) could be launched from a 200-caliber-long launch tube at 25,000 ft/sec using helium as a propellant. It was desired that the largest possible diameter launch tube be used in order that winged or sub-caliber models could be launched within the weight limitation assumed. Since the performance is nearly independent of size, the upper limit of dimensions was expected to be fixed by cost, the distance between already installed foundations, space in the launch room, or availability of excess gun tubes which could be used.

IDEAL PERFORMANCE OF THE TWO-STAGE SYSTEM

The following simplified model of the two-stage launcher system is assumed as a first approximation to estimate the performance. Initial conditions in the chamber are such that the piston arrives near the end of the pump tube with a velocity given by conventional interior ballistic theory. A shock is driven ahead of the piston which reflects from the end of the pump tube and from the piston face. Compression after the three shock passages is taken to be isentropic to a final state which results from conversion of the kinetic energy of the piston into an increase of the internal energy of the compressed gas in the pump tube. This gas is the propellant which drives the projectile through the launch tube. It is implied that the piston comes to rest before the projectile starts and that it stays fixed during projectile motion. In the following section, semi-empirical limits are imposed to restrict the initial motion of the projectile and to limit a falling pressure resulting from the reversal of a light piston. An ideal gas is assumed (γ = const.), and no losses through friction or heat transfer are admitted.

COMPRESSION PROCESS IN A PUMP TUBE

When gas in state (1) (see Fig. 1) is driven ahead of a relatively fast moving piston, a shock wave runs ahead of the piston. The pressure ratio across the shock wave is related to the piston velocity by

$$\left(\frac{u_p}{a_1}\right)^2 = \frac{2}{\gamma(\gamma+1)} \frac{\left(\frac{P_2}{P_1} - 1\right)^2}{\left(\frac{P_2}{P_1} + \frac{\gamma-1}{\gamma+1}\right)}$$

and the temperature ratio is given by

$$\frac{T_2}{T_1} = \frac{\frac{P_2}{P_1}}{\frac{P_2}{P_1} + \frac{\gamma-1}{\gamma+1}} \left(1 + \frac{\gamma-1}{\gamma+1} \frac{P_2}{P_1}\right)$$

If the end of the pump tube is closed, the shock will reflect leaving a state (3) of higher pressure and temperature and zero velocity. This reflected shock will again reflect from the piston face, which is assumed to be traveling at its original speed, resulting in the conditions (4) (Fig. 1 for helium). For an infinitely massive piston, the shock wave

will continue to be reflected from the end of the pump tube and piston face. These shocks have in common the velocity change across them equal to the piston speed, u_p. However, since the acoustic speed is continuously increasing, the shock Mach number becomes progressively smaller, the shock compression approaches an isentropic process, and the difference between shock and isentropic compression after the first three shock transits is very small. When the piston mass is finite, the shock first reflected from it weakens as a result of the piston's deceleration, thereby insuring an even more nearly isentropic process during the final compression stage. Figure 2 shows the compression process for multiple shocks (up to 6) with constant piston speed and also shows compression through three shocks followed by an isentropic compression to the same pressure as obtained with the 6-shock compression. This consideration leads to the following simple relation between shock and isentropic compression for pump tubes:

$$\frac{T_{F\,Shock}}{T_{F\,Isentropic}} = \frac{\frac{T_4}{T_1}}{\left(\frac{P_4}{P_1}\right)^{\frac{\gamma-1}{\gamma}}} = f\left(\frac{u_p}{a_1}\right)$$

shown in Fig. 3 for helium.
Therefore, if the final pressure can be determined for a given piston velocity, the final state (F) of the gas in the pump will be known (Ref. 2).

FINAL PRESSURE IN THE PUMP TUBE

The wave plane (distance-time) representation of the pump tube shows the relationship graphically:

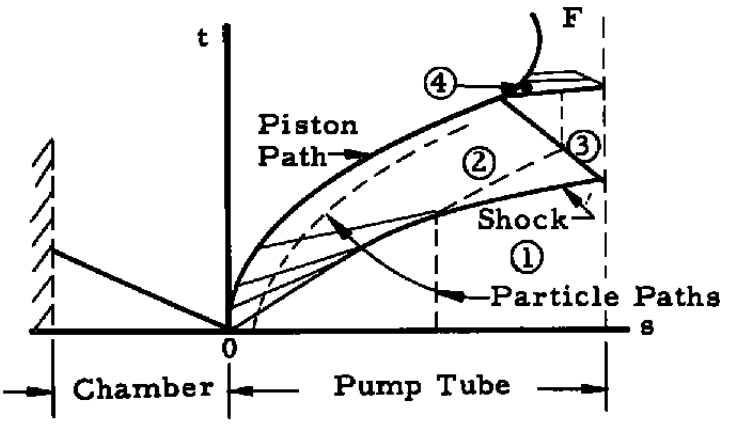

Region (1) is the undisturbed gas in the pump tube, (2) is assumed to be uniform in the present quasi-steady analysis, (3) results when the

shock is reflected from the pump tube end, and (4) from the piston face. In reality region (2) is not uniform as can be seen from the particle paths -- the compression corresponds to the incident shock at the front of the region, whereas it is isentropic at the piston face. Light piston weight and long pump tube length give better conformity to the quasi-steady assumption. A final state (F) is attained when the piston comes to rest.

It is assumed (a) that the driven gas undergoes an entropy change corresponding to the shock compressions to state (4) followed by an isentropic compression to the final state (F) and (b) that the kinetic energy of the piston is equal to the change in internal energy from the rest state (3) to the final state (F). This is

$$\frac{1}{2} m_p u_p^2 = \Delta e = C_v (T_F - T_3) \rho_1 A_p \ell_p$$

Isentropic compression from (4) to (F),

$$\frac{T_F}{T_4} = \left(\frac{P_F}{P_4}\right)^{\frac{\gamma-1}{\gamma}}$$

Then

$$\frac{m_p u_p^2}{2 \rho_1 A_p \ell_p} = C_v T_4 \left[\left(\frac{P_F}{P_4}\right)^{\frac{\gamma-1}{\gamma}} - \frac{T_3}{T_4}\right]$$

or

$$\frac{P_F}{P_4} = \left[\frac{m_p u_p^2}{2 C_v T_4 \rho_1 A_p \ell_p} - \frac{T_3}{T_4}\right]^{\frac{\gamma}{\gamma-1}}$$

and

$$\frac{P_F}{P_1} = \frac{P_4}{P_1}\left[\frac{\gamma-1}{2} \bar{M} \frac{\left(\frac{u_p}{a_1}\right)^2}{\frac{T_4}{T_1}} + \frac{T_3}{T_4}\right]^{\frac{\gamma}{\gamma-1}} = f\left(\frac{u_p}{a_1}, \bar{M}\right)$$

where the dimensionless piston mass ($\bar{M}$) is defined as

$$\bar{M} = \frac{m_p a_1^2}{P_1 A_p \ell_p}$$

which is proportional to the ratio of piston mass to pump tube charge mass.

The above relation between final pressure, piston velocity, and piston mass permits the construction of a general pump tube performance chart in which the final pressure ratio and acoustic speed are functions of piston mass and velocity (Fig. 4a). Figure 4b is the ratio of final to initial volume in the pump tube.

$$\frac{V_F}{V_i} = \frac{\frac{T_F}{T_i}}{\frac{P_F}{P_i}}$$

The final volume is a chamber for the launch tube and will therefore adversely influence the projectile velocity if it is below a minimum amount.

PISTON VELOCITY

In Ref. 2, the method for estimating the velocity of a piston in the pump tube is developed. The chamber is assumed to be large enough to permit computation of the piston rear face pressure from the unsteady flow analysis for no-chambrage, infinite chamber length geometry. In dimensionless form this is

$$\bar{P}_R = \left[1 - \frac{\gamma - 1}{2} \bar{u}_p\right]^{\frac{2\gamma}{\gamma-1}}$$

$$\bar{P}_R = \frac{P_R}{P_c} \quad \text{and} \quad \bar{u}_p = \frac{u_p}{a_c}$$

where the subscript (c) refers to chamber conditions.

The forward face pressure is given by

$$\bar{P}_f = \bar{P}_i \left[1 + \frac{\gamma_i}{2} \frac{\bar{u}_p}{\bar{a}_i} \left(\frac{\gamma_i + 1}{2} \frac{\bar{u}_p}{\bar{a}_i} + \sqrt{4 + \left(\frac{\gamma + 1}{2} \frac{\bar{u}_p}{\bar{a}_i}\right)^2}\right)\right]$$

The subscript (1) refers again to the undisturbed conditions ahead of the piston. Then the piston velocity-travel relationship is given by the integral,

$$\bar{s}_p = \int_0^{\bar{u}_p} \frac{\bar{u}\, d\bar{u}}{\bar{P}_R - \bar{P}_f}$$

where

$$\bar{s}_p = \frac{P_c A_p s}{m_p a_c^2}$$

The dimensionless piston speed-distance function is given in Fig. 5 for a chamber propellant derived from 100-percent combustion of hydrogen and oxygen in helium, the mixture being $3H_2 + O_2 + 8He$ (Ref. 3).

Using the piston velocity obtained from the foregoing, it is possible to obtain another form of the generalized pump tube performance curves more suitable for the present purpose, i. e., optimization of the complete launch system. The final pressure and acoustic velocity in the pump tube were shown to be functions of piston speed (u_p/a_i) and mass parameter $(\bar{M})$. By defining another mass parameter:

$$C = \frac{\frac{a_i^2}{P_c}\,\frac{m_p}{A_p d_p}}{\left(\frac{\ell}{d}\right)_p}$$

some of the physical variables are brought out more distinctly. The piston density is $\frac{m_p}{A_p d_p}$, and the pump tube fineness ratio is $\left(\frac{\ell}{d}\right)_p$

where

$$\frac{u_p}{a_i} = \frac{a_c}{a_i} f(\bar{s}_p)$$

$$\bar{s}_p = \frac{\left(\frac{a_i}{a_c}\right)^2}{C} \qquad \text{(piston travel = pump tube length)}$$

$$\bar{M} = \left(\frac{P_c}{P_i}\right) C$$

and therefore,

$$\frac{P_F}{P_c} = \left(\frac{P_F}{P_i}\right)\left(\frac{P_i}{P_c}\right) = \frac{P_i}{P_c} f\left(\bar{M}, \frac{u_p}{a_i}\right) = f\left(\frac{P_i}{P_c}, C\right)$$

for fixed a_i/a_c . Figure 6 shows these functions for a pump tube charge temperature of 300°K and chamber acoustic velocity of 7150 ft/sec, which corresponds to the $H_2 - O_2 - He$ combustion products. When the chamber pressure is assumed to be fixed by practical considerations, the effects of varying piston mass and pump tube initial charge pressure (P_i) are clearly evident. The high pressures that occur when piston mass is large or charge pressure low have been observed by all those who have experimented with this type of launcher. It is to be expected that low piston weight will produce higher projectile velocities for a limiting level of final pressure. Figure 6 is possible because of the unique relation between chamber pressure and acoustic speed. For other types of first stages (gunpowder - helium for instance), final conditions must be determined as in Fig. 4.

LAUNCH TUBE PERFORMANCE

The velocity of the projectile when it leaves the evacuated launch tube depends upon the state of the gas compressed in the pump tube, the geometry of the launch tube, and final volume. For a fixed geometry, the following dimensionless parameters describe launch performance:

$$\bar{u}_M = \frac{u_M}{a_F} = f(\bar{s}_L) \quad \text{(model velocity at launch)}$$

$$\bar{t}_L = \frac{P_F A_L}{m_M a_F} t = f(\bar{s}_L) \quad \text{(time in launch tube)}$$

where the dimensionless distance is given by

$$\bar{s}_L = \frac{P_F A_L}{m_M a_F^2} \ell_L$$

A simple reference case which has a closed form solution for $\bar{u}$ and $\bar{t}$ is possible when the chamber is infinitely long and has the same diameter as the launch tube. This is the same as for the piston discussed before except that the forward face pressure (P_f) is zero.

$$\bar{s} = \int_0^{\bar{u}} \frac{\bar{u}\, d\bar{u}}{\left[1 - \frac{\gamma-1}{2}\bar{u}\right]^{\frac{2\gamma}{\gamma-1}}} = \frac{2}{\gamma-1}\left\{\frac{\frac{2}{\gamma+1} - \left[1 - \frac{\gamma-1}{2}\bar{u}\right]}{\left[1 - \frac{\gamma-1}{2}\bar{u}\right]^{\frac{\gamma+1}{\gamma-1}}} + \frac{\gamma-1}{\gamma+1}\right\}$$

and

$$\bar{t} = \int_0^{\bar{u}} \frac{d\bar{u}}{\left[1 - \frac{\gamma-1}{2}\bar{u}\right]^{\frac{2\gamma}{\gamma-1}}} = \frac{\frac{2}{\gamma+1}}{\left[1 - \frac{\gamma-1}{2}\bar{u}\right]^{\frac{\gamma+1}{\gamma-1}}} - \frac{2}{\gamma+1}$$

(see Fig. 7)

The more general case for which the chamber length is finite and its diameter is larger than the launch tube is treated in Ref. 2. The method of characteristics was used to obtain solutions applicable to helium as a propellant for chambrage (ratio of chamber area to launch tube area) of 1 and 4 and various chamber lengths. The results are summarized in Fig. 8 as the effect of chamber volume to launch tube volume on the launch velocity normalized to the reference velocity in Fig. 7. Corresponding to the pump tube final acoustic velocity and pressure, the reference velocity of launch can be determined from Fig. 7, and the correction of Fig. 8 applied for the ratio of final volume to launch tube volume. It will be observed that the effects of chambrage and finite chamber length nearly compensate for each other when the chamber volume is held fixed.

FACTORS INFLUENCING ACTUAL PERFORMANCE

The ideal performance of the two-stage launcher discussed in the previous section neglects two major effects which tend to reduce the actual velocity below the calculated. First, the piston has been assumed to come to rest and stay fixed before the projectile starts to move. If the piston has a low mass relative to the projectile, it will reverse its direction and cause a drop in pressure driving the projectile. The second factor that may adversely affect launch velocity is the result of the projectile's having moved far down the launch tube before the pump tube pressure reaches a maximum. In order to avoid break-up of the projectile if it were subjected to the peak pressure, it is usually restrained by a light shear diaphragm which fails when the first shock reflects from the pump tube end. A lower base pressure results without serious loss in propelling work if the initial projectile travel is only a small fraction of the launch tube length. These effects are shown qualitatively on the following s-t plane

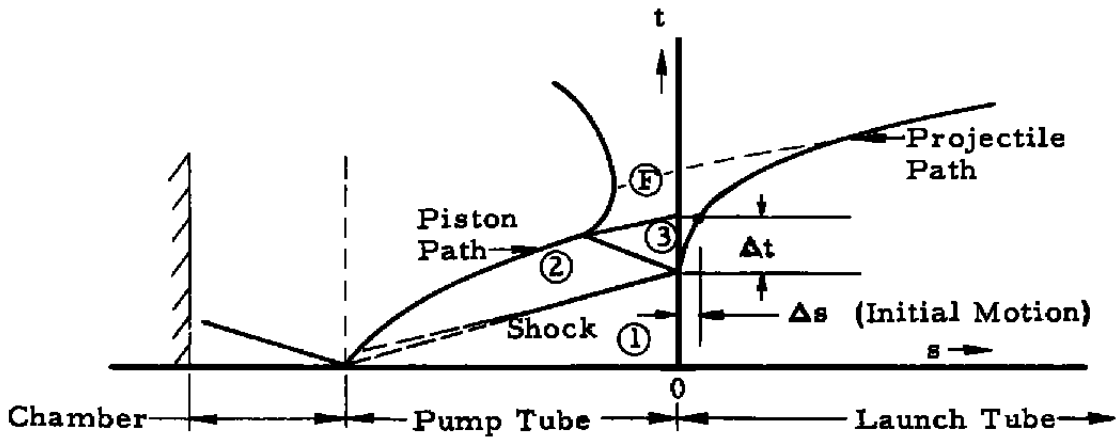

The rigorous solution of the above motions is prohibitively complex, and an empirical approach is resorted to, based upon operating experience with this type of launcher and simple physical models. Experimental data are available for a variety of piston and projectile masses which give an insight into the piston reversal effect and for two pump tube lengths which show the effect of initial projectile motion.

PISTON REVERSAL (Piston Mass Parameter)

For the derivation of a parameter associated with the piston reversal effect, the following model is used:

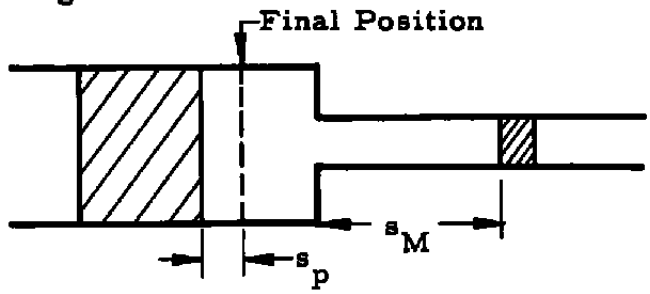

The piston is considered to be accelerating back under the influence of the final pressure (P_F) and the motion of the projectile assumed not to affect the pressure. The early stages of motion are given by the dimensionless time and distance functions of Fig. 7 (Ref. 2).

$$s_p = \frac{m_p a_f^2}{P_F A_F} f\left(\frac{P_F A_P}{m_p a_f^2} t\right)$$

and the projectile motion is given by

$$s_M = \frac{m_M a_F^2}{P_F A_L} f\left(\frac{P_F A_L}{m_M a_f} t\right)$$

It is desirable to refer the piston motion to the non-dimensional projectile motion defined by

$$\bar{s} = \frac{P_F A_L}{m_M a_F^2} s \qquad \text{and} \qquad \bar{t} = \frac{P_F A_L}{m_M a_F} t$$

Then

$$\bar{s}_p = \frac{m_p A_L}{m_M A_p} f\left(\frac{m_M A_p}{m_p A_L} \bar{t}\right)$$

where $f = \bar{s}(\bar{t})$ (Fig. 7)
Considering the pressure decay of the piston face,

$$\frac{P_p}{P_F} = \left[1 - \frac{\gamma - 1}{2} \frac{u_p}{a_F}\right]^{\frac{2\gamma}{\gamma - 1}}$$

where

$$\frac{u_p}{a_f} = f\left(\frac{P_F A_p}{m_p a_f^2} s_p\right) = f\left(\frac{m_M A_p}{m_p A_L} \bar{s}_p\right)$$

where $f = \bar{u}(\bar{s})$ (Fig. 7)

It is evident that the controlling factor is the parameter $\left(\frac{m_p A_L}{m_M A_p}\right)$. In Fig. 9, the pressure drop and relative motion of piston and projectile are shown for a range of mass parameter typical of two-stage launchers. These results must be considered as only qualitative since there is a time delay in communicating the falling pressure from the piston to the projectile along downstream characteristic lines. Comparison of measured to calculated launch velocities provides a correlation with the mass parameter which will permit some reasonable lower limit to be set for design purposes.

PROJECTILE INITIAL MOTION

The projectile will usually begin to move under the force of the first reflected overpressure (P_3) when the incident shock arrives at the end of the pump tube. A rigorous computation of the distance the projectile moves before the pressure maximum occurs is difficult; however, a simple analysis is possible which shows the fundamentals of the phenomenon. The wave plane is shown below:

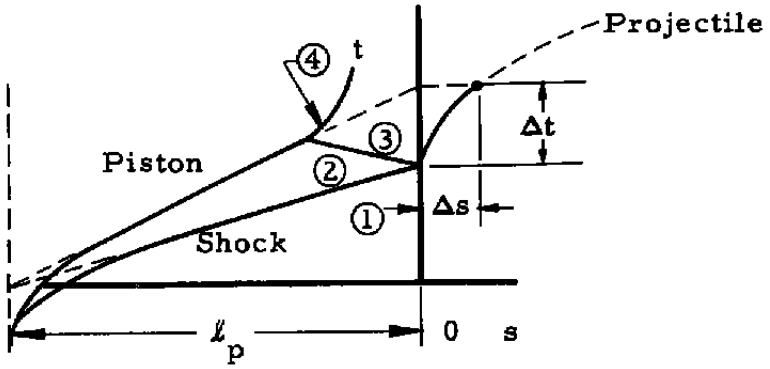

The time interval (Δt) between the arrivals of the two first shocks is taken as the essential measure of the problem. It is assumed (a) that the incident shock and projectile path have constant speeds originating at the beginning of the pump tube and (b) that the shocks (2) – (3) and (3) – (1) are straight. Measurements of the time between the arrival of the first shock and peak pressure are in reasonable agreement with the above simplification.

Referring to the diagram above, the shock speeds (u_{s_1}, u_{s_2}, and u_{s_3}) refer to the incident, first reflected, and second reflected waves. The time of arrival of the incident shock is

$$t_1 = \frac{\ell_p}{u_{s_1}}$$

and at this time the piston is at the location ($s_{p_1} = u_p t_1 - \ell_p$). The time interval ($\Delta t$) between shock arrivals at the end of the pump tube is

$$\Delta t = \frac{-s_4}{u_{s_2} - u_p} + \frac{-\bar{s}_4}{u_{s_3}} = -s_{p_1}\left(1 - \frac{u_p}{u_{s_2}}\right)\left(\frac{1}{u_{s_2} - u_p} + \frac{1}{u_{s_3}}\right)$$

$$= \ell_p \left(1 - \frac{u_p}{u_{s_1}}\right)\left(1 - \frac{u_p}{u_{s_2}}\right)\left(\frac{1}{u_{s_2} - u_p} + \frac{1}{u_{s_3}}\right)$$

$$= \frac{\ell_p}{a_1} f_{\Delta t}\left(\frac{u_p}{a_1}\right)$$

The shock velocities are given by

$$\frac{u_p}{a_n} = 1 - \left(\frac{\gamma - 1}{\gamma + 1}\right)\left(\frac{u_{s_n}}{a_n} - \frac{a_n}{u_{s_n}}\right) \quad (n \text{ indicates the n-th shock})$$

The dimensionless function of u_p/a_1 can be readily calculated for an ideal gas and is shown in Fig. 10 for helium.

The initial motion of the projectile is the result of the reflected shock conditions (3). This is derived from the interior ballistics analysis as in Fig. 7.

$$\Delta s_M = \frac{m_M a_3^2}{P_3 A_L} f_t\left(\frac{P_3 A_L}{m_M a_3} \Delta t\right) \qquad f_t = \bar{s}(\bar{t})$$

$$\Delta u_M = a_3 f_u\left(\frac{P_3 A_L}{m_M a_3^2} \Delta s\right) \qquad f_u = \bar{u}(\bar{s})$$

These will be non-dimensionalized to the form which can be compared to the coordinates discussed previously, i. e.

$$\bar{u} = \frac{u}{a_F}, \quad \bar{s} = \frac{P_F A_L}{m_M a_F^2} s, \text{ and } \bar{t} = \frac{P_F A_L}{m_M a_F} t$$

Then

$$\Delta \bar{t} = \bar{\ell}_p \left(\frac{a_F}{a_1}\right) f_{\Delta t}\left(\frac{u_p}{a_1}\right)$$

$$= \frac{\ell_p}{\ell_L} \bar{s}_L \frac{a_F}{a_1} f_{\Delta t}\left(\frac{u_p}{a_1}\right)$$

$$\Delta \bar{s}_M = \frac{P_F}{P_3}\left(\frac{a_3}{a_F}\right)^2 f_t\left(\frac{P_3}{P_F}\frac{a_F}{a_3} \Delta \bar{t}\right)$$

The criterion for correlation of the effect of initial projectile motion is taken as

$$\frac{\Delta s}{\ell_L} = \frac{\Delta \bar{s}}{\bar{s}_L}$$

which is approximately the fraction of the launch tube traversed by the projectile before peak pressure is obtained in the pump tube.

EVALUATION OF EXPERIMENTAL RESULTS

An essential aspect of the present analysis of two-stage launcher performance is the empirical evaluation of the effects of initial projectile motion and piston reversal. A launcher was assembled using as the first stage a 40-mm, H_2-O_2-He configuration of NOL design. Pump tube lengths were 20.5 ft and 10.5 ft with a diameter of 1.58 in. Initially, a 20-mm launch tube liner was used; however, calculations of final volume indicated that the pump tube was too small. Therefore, 0.50-in.-bore launch tubes 8 to 13 ft in length were used in all the tests. During the program of testing, preliminary hydrogen thermodynamic data became available from the Bureau of Standards, which made it possible to compute launcher performance similarly to the method for helium outlined. Much lower final temperatures resulted for hydrogen compared with helium, and it was found that the effect of final temperature in the pump tube could be isolated.

The chamber pressure upon which piston velocity is based is measured with a Norwood bonded strain-gage pressure transducer. During the program, development of high-pressure section pressure gages progressed to the point that the last few tests included a strain-gage tube type that could be calibrated to 185,000 psi. Also, Rodman copper crusher gages appeared to give reasonable results when the piston area was reduced so that tarage table calibration was applicable. Sufficient data are not yet available to verify theoretical determination of maximum pressures; however, strain gages on the outside of the high pressure section and measurements of yielding of the bore are consistent with the calculated pressure. Recording of chamber pressure was done on a Midwest oscillograph with galvanometers having about 300-cps frequency response. Time resolution was about 0.2 msec on the paper traces.

Velocity measurement was based on four independent systems: (1) a Beckman-Whitley Model 192, high-speed framing camera with 0.1-percent or better velocity determination, (2) light detector trigger units whose output was displayed on a scope with about 2-percent resolution, (3) spark shadowgraphs from stations 45 ft apart -- 10-megacycle

counters were used to determine the interval between sparks, and (4) four to six wire grids distributed along the 100-ft range, the outputs of which were used to start and stop counters. In addition, an independent time base was established for the sparks and break wires by use of tape recording and slow playback which permits time resolution of about 3 microseconds. At least two independent methods were required for the round to be considered successful.

In Table 1, a series of rounds is given in which most of the physical parameters of the launcher are varied. Measured launch velocities are compared with those computed to provide a basis for correlation. Piston velocities were calculated for the fraction of complete combustion determined from chamber pressure by a method similar to that of Ref. 3. The initial projectile motion $\left(\frac{\Delta s}{\ell_L}\right)$, piston reversal parameter $\left(\frac{m_p A_L}{m_M A_p}\right)$, and final temperature are tabulated. Figure 11a shows the ratio of measured to calculated launch velocity as a function of each of these quantities.

Careful examination of Fig. 11a reveals trends that are not superficially obvious. The rounds in which hydrogen was the propellant were affected almost solely by the initial projectile motion $\left(\frac{\Delta s}{\ell_L}\right)$ since the final temperature was low (2000 to 3000°K) and the piston mass parameter was well above 3. The group of rounds, 140 to 143, were characterized by a low piston reversal parameter. Although the trend was not adequately defined, the lowest velocity ratio also has the lowest value of the parameter. The remainder of the helium rounds had a wide range of final temperatures and initial motion parameter. The former appeared to have the dominant effect, either through heat transfer from the propellant or because of contamination from vaporizing the walls of the launcher. A simple empirical formula of the following form was deduced, with T_F in °K,

$$\frac{u}{u_{calc}} = 1 - \frac{0.4}{\left(\frac{m_p A_L}{m_M A_p}\right)^2} - 7.4 \left(\frac{\Delta s}{\ell_c}\right)^2 - 3\,(T_F - 2000) \times 10^{-5}$$

This was then applied to the calculated data and compared with the experimental results as shown in Fig. 11b. Lines of 10-percent deviation from the correlation are given, indicating that most of the points fall within about 6 percent. There is a reasonable explanation for most of those points which show a large deviation from the correlation: (a) No. 142 and 143 projectiles were made of aluminum and had a shear out strength

which was appreciably higher than any of the other rounds -- the initial projectile motion may thereby have been restricted, (b) No. 146 had a very high maximum pressure (P_f > 300,000 psi) , and the high pressure seal failed tending to lower launch velocity, (c) No. 154 was the only round to have a plastic entrance to the launch tube, and it is believed that ablation of this element contributed to low velocity, and (d) No. 156 is an anomaly in that the recorded chamber pressure (upon which the calculated velocity was based) indicated more pressure than would be provided by 100-percent combustion in a closed chamber. In calculating the velocity, 100-percent combustion was assumed. It is suspected that the transducer calibration was erroneous and that the calculated velocity was too high.

Table 2 is an attempt to correlate the NASA Ames launcher (Ref. 1) by the same empirical formula that was derived from the AEDC data. The proportions of the former are more favorable because of its larger pump tube and initial projectile motion was always less than 10 percent of the launch tube length. The correlation formula developed above was applied to the data with the results shown in Fig. 12. In the calculated performance of the Ames launcher, it was assumed that the piston velocity was related to chamber pressure as if 100-percent combustion of a H_2-O_2-He mixture were used. Rodman gages were used to obtain chamber pressures, and an average of readings at each end of the chamber was taken for the calculations. The actual piston velocity, repeatability and accuracy of the gage readings are not known. Round No. 91, which is far off the correlation line, had only half the piston reversal parameter $\left(\frac{m_p A_L}{m_M A_p}\right)$ of the lowest value used in the formula derivation. It is therefore probable that the second term overestimates the piston reversal effect at very low values of $\frac{m_p A_L}{m_M A_p}$.

The fact that the empirical formula permits predicting the performance within 10 percent for the AEDC launcher with a large variation in geometry and also for the Ames Research Center configuration, which has an appreciably different configuration, leads to the conclusion that the magnitudes of all the important physical variables have been determined. It is immediately apparent that limits can be set for design of this type of launch system. If the deleterious effects of piston reversal and initial projectile movement are each to be limited to one percent of launch velocity, the parameters, $\left(\frac{m_p A_L}{m_M A_p}\right)$ must exceed 6 and $\left(\frac{\Delta s}{\ell_L}\right)$ must be less than 0.1. Because of the strong adverse effect of raising

propellant temperature, the attainment of much higher velocities using helium does not appear promising. On the other hand, the temperature of hydrogen can be raised by a factor of two with only about a 10-percent loss in velocity resulting from heat transfer phenomena. Therefore, a potential of about 30-percent increase over currently achieved maximum velocity may be anticipated with the two-stage launcher configuration.

DESIGN PROCEDURE FOR LAUNCHER

The design of the large scale launcher was based upon duplicating or slightly improving the performance of the most successful of the small scale launchers now in operation. This performance is represented by the launcher described in Ref. 1 and is approximately as follows: launch velocity of 24,000 ft/sec of a one-half caliber length plastic projectile using helium in a 265-caliber length launch tube. The following criteria were therefore used to evolve a conservative design configuration:

a. Projectile, 1-caliber plastic; specific gravity, 1.15
b. Launch Tube, 200-caliber length
c. Launch Velocity, 25,000 ft/sec
d. Propellant, helium

Further considerations were to keep the pressures low enough to avoid the use of exotic structural materials, overall length compatible with the existing foundations in the "G" Facility launch room, and the possible use of available ordnance tubes.

From the preceding analysis it is evident that geometrical similarity (including piston and projectile) equal pressures, and the same density of piston and projectile will result in the same launch velocity independent of scale. The same is true of stress level and the structural design. It is therefore necessary only to determine a satisfactory geometry, then to scale it up to the largest launch tube size compatible with space requirements and operational practicability. A large launch tube is particularly desirable for winged models and for obtaining increased launch velocities with small models.

The effects of chamber pressure (assuming a combustion H_2-O_2-He mixture), piston mass, and pump tube length-diameter ratio are computed by the methods previously developed, and comparisons of the resulting maximum pressure, initial projectile motion, and weight of the driving section (chamber and high pressure section) are made. The piston mass

parameter $\left(\frac{m_p A_L}{m_M A_p}\right)$ is fixed at 3 to limit the adverse effect of piston reversal. The projectile initial motion parameter $(\Delta s/\ell_L)$ is limited to 0.1 on the basis of the foregoing experimental results.

LAUNCH TUBE REQUIREMENTS

Figure 6a shows final pump tube conditions (a_F/a_i vs P_F/P_c) corresponding to various piston mass and pump tube charge parameters,

$$C = \frac{\frac{a_i^2}{P_c}\,\frac{m_p}{A_p d_p}}{\left(\frac{\ell}{d}\right)_p} \quad \text{and} \quad \frac{P_i}{P_c}$$

The launch tube requirements will be expressed in the same coordinate system, and by superposing, the pump tube is matched to the launch tube. The reference launch velocity, (u_o – no chambrage, infinite chamber length), is shown in Fig. 7. In dimensionless form,

$$\frac{u_o}{a_F} = f(\bar{s}_L) = f\left(\frac{P_F A_L \ell_L}{m_M a_F^2}\right)$$

or

$$\bar{s}_L = \frac{P_F}{a_F^2}\,\frac{A_L d_L}{m_M}\left(\frac{\ell}{d}\right)_L$$

in a more convenient grouping of terms. For the case considered $(\ell/d)_L = 200$ and $m_M/A_L d_L = 1.15$ gm/cc. Figure 13 shows the relationship between a_F and P_F required to produce the launch velocities, 22,000, 24,000 and 25,000 ft/sec. The several velocities are chosen in order that the desired velocity of 25,000 ft/sec can be determined by interpolation after the effect of finite chamber geometry is determined from the final volume ratio (V_F/V_i) (Fig. 8). By selecting two chamber pressures (P_c = 15,000 and 25,000 psi), Fig. 13 is converted into the coordinates of Fig. 6, and the values of C and P_i/P_c determined at the intersection with the constant (C) lines. The corresponding values of the following quantities are then readily determined:

$$C\,,\quad \frac{a_F}{a_i}\,,\quad \frac{V_F}{V_i}\,,\quad P_F\,,\quad \text{and}\quad \frac{u_p}{a_i}$$

The piston mass density ($m_p/A_p d_p$) is fixed, and the pump tube fineness ratio is

$$\left(\frac{\ell}{d}\right)_p = \left(\frac{m_p}{A_p d_p}\right)\,\frac{a_i^2}{P_F}\,\frac{1}{C}$$

The size of the pump tube (d_p/d_L) is next determined based on the empirical piston reversal parameter:

$$\frac{m_p A_L}{m_M A_p} = 3$$

$$\frac{d_p}{d_L} = \frac{3\left(\frac{m_M}{A_L d_L}\right)}{\frac{m_p}{A_p d_p}}$$

or alternately upon the requirement that the final volume (V_F) is large enough to produce a velocity of 25,000 ft/sec; i.e. V_F/V_L corresponds to $u/u_o = 1$ (Fig. 8).

$$\frac{d_p}{d_L} = \sqrt[3]{\frac{V_F}{V_L}\,\frac{\left(\frac{\ell}{d}\right)_L}{\left(\frac{\ell}{d}\right)_p\ \left(\frac{V_F}{V_i}\right)}}$$

The larger of the two values is chosen; if the pump tube diameter were based on the first criterion, u/u_o would be different from 1. In this case, an interpolation is made to find the conditions corresponding to the required launch velocity of 25,000 ft/sec. The calculation of initial projectile movement ($\Delta s/\ell_L$ and P_F) as functions of pump tube length/diameter ratio is made as previously discussed.

EFFECT OF PHYSICAL VARIABLES

In order to arrive at a comparison of configurations based on cost, the volume of the driver section (chamber, pump tube, and high-pressure section) in terms of launch tube volume is computed. The wall thickness is based on Fig. 14 where the ratio of internal pressure to maximum tangential stress is shown as a function of OD/ID for two-dimensional cylinders with an optimum two-shell shrink fit assembly. A yield stress of 120,000 psi is assumed, and the pressure in the chamber and pump tube is 25,000 psi. The length of the high-pressure section of the pump tube is based on the volume ratio (V_F/V_i). This gives the following formula:

$$\frac{V_{driver}}{V_L} = \left(\frac{d_p}{d_L}\right)^3 \left\{ \frac{\left(\frac{\ell}{d}\right)_p}{\left(\frac{\ell}{d}\right)_L} \frac{V_F}{V_i} \left[\left(\frac{d_o}{d_L}\right)^2_{p_F} - 1\right] + \frac{\left(\frac{\ell}{d}\right)_p}{\left(\frac{\ell}{d}\right)_L} \left[\left(\frac{d_o}{d_i}\right)^2_{25{,}000\ psi} - 1\right] \right.$$

$$\left. + \frac{\left(\frac{\ell}{d}\right)_c}{\left(\frac{\ell}{d}\right)_L} \left[\left(\frac{d_o}{d_i}\right)^2_{25{,}000\ psia} - 1\right] \left(\frac{d_o}{d_p}\right)^3 \right\}$$

In Figs. 15 and 16, the results of the foregoing calculations are presented for piston densities, $m_p/A_p d_p$ = 0.86 and 1.15 gm/cc, and chamber pressures, P_c = 15,000 and 25,000 psi. The axis of abscissas is length/diameter ratio of the pump tube.

SELECTION OF LAUNCHER CONFIGURATION

Examination of Figs. 15 and 16 shows a shaded region in which the desired performance can be obtained. Figure 15 is for the minimum weight piston* and Fig. 16 for 1-1/3 times the minimum weight. The boundaries of the region are taken as an initial projectile motion of 10 percent of the launch tube length and a peak pressure of 200,000 psi. Chamber pressures of 15,000 and 25,000 psi are considered a reasonable operating range. In general, longer pump tubes and lighter pistons result in lower peak pressures, but greater initial motion of the projectile. Pump tubes (ℓ/d) from 48 to about 60 are acceptable with the lightest piston and only 80 with the heavier. The pump tube diameter to launch tube diameter ratio is 4 for the light piston and 3 for the heavy piston in order to provide a piston mass parameter $\left(\frac{m_p A_L}{m_M A_p}\right)$ of 3. The pump tube would from 192 to 240 launch tube diameters for the light piston and 240 for the heavier one, so that the former would result in a shorter overall launcher. The weight of the driver (chamber + pump tube) is twice that for the heavier piston configuration, however. The cost of the light piston version would therefore be about twice as much for the driver section. A further increase in piston weight would not be practicable because of the limitation on chamber pressure, which cannot be closely controlled. The limits for the desired configuration therefore fall between 190 and 240 launch tube diameters for the pump tube length, and piston weight between 0.75 and 1 caliber length plastic. The pump tube bore should be three to four times the launch tube bore.

The availability of 8-in. Naval rifle liners, which had been autofrettaged to about 60,000 psi, made it attractive economically to design around them as a pump tube. An $(\ell/d)_p$ of 52.75 is possible, which falls within the desirable range for a 2-in.-diam launch tube and the minimum weight piston. A 120-gm projectile could therefore be launched from a 200-caliber launch tube at 25,000 ft/sec using helium as a propellant.

---

*A minimum weight piston is assumed to have the mass/area of a 0.75-caliber length plastic cylinder. This limit is based upon experience with stability and structural integrity of projectiles of high velocity.

It was decided however to construct the launcher with a 2.5-in. -bore launch tube (Fig. 17) which would result in lower velocity. But since it is known that an appreciable increase in performance will result from the use of hydrogen as a propellant and that an increase in length of the launch tube to 250 or more calibers, acceptable velocities would be attained.

ESTIMATED PERFORMANCE OF THE LAUNCHER

Figure 18 shows the launch velocities calculated for the 200-caliber, 2.5-in. launch tube using helium. Here the effects of piston weight, chamber pressure, and fraction of complete combustion are evident. As a conservative nominal performance for a maximum pressure of 200,000 psi (the chamber pressure is taken as 20,000 psi, charge pressure 200 psi, piston 1-caliber plastic, and combustion 75-percent), a launch velocity of 23,000 ft/sec is anticipated. With a 0.75-caliber piston and 100-percent combustion, 24,000 ft/sec is obtained. As the boundary ($\Delta s/\ell_L$) is crossed with increasing charge pressure, the velocity will be less than shown as indicated in Fig. 11.

The actual launcher will use gunpowder - heated helium or hydrogen in the chamber. Preliminary experiments and Ames Center and AEDC data indicate that the same piston velocities are obtainable with gunpowder - heated helium as with the H_2-O_2-He first stage.

CONCLUDING REMARKS

A 2.5-in. -bore launcher has been designed capable of launching a 230-gm projectile in excess of 20,000 ft/sec. This launcher will be installed in the Arnold Center 1000-ft aeroballistic range designated Facility "G" of the von Kármán Gas Dynamics Facility. The design is considered to represent the present state of development of model launchers. Electrical energy augmentation systems presently under study on Air Force contracts may provide means for appreciably improving launch velocities. These methods rely on use of a launcher of the type discussed here as the basic equipment to which augmentation stages are added. It appears, therefore, that the present design not only fulfills the requirement for the initial launcher, but provides for growth potential.

The use of helium in the performance computations is considered to be conservative in that two simple methods of improving the launch

velocity are available. The substitution of hydrogen for helium in the pump tube yields between 10 and 20 percent increase in velocity. Study of the effect of pre-heating helium to 600°K in the pump tube indicates that from 10 to 15 percent more velocity may be obtained (the maximum pressure being the same in both cases). In addition, there is evidence that increasing launch tube length beyond 200 calibers will result in higher launch velocities (at least up to 250 calibers).

The effect of final temperature has not been included in the performance estimates for the launcher (shown in Fig. 18) and the experimental correlation referred to indicates that a velocity loss up to 15 percent will occur if helium is used as the propellant.

REFERENCES

1. Bioletti, C. and Cunningham, B. E. "A High Velocity Gun Employing a Shock Compressed Light Gas." NASA TN D-307, February 1960.
2. Stephenson, W. G. "Theoretical Light Gas Gun Performance." AEDC-TR-61-1, May 1961.
3. Lord, M. E. "Performance of a 40-mm Combustion Heated Light Gas Gun Launcher." AEDC-TN-60-176, October 1960.

TABLE 1

EXPERIMENTAL RESULTS FROM 0.5-CALIBER, TWO-STAGE LAUNCHER

Round	ℓ_p ft	ℓ_L ft	m_p g	m_M g	P_c psi	P_1 psia	$u_{(exp)}$ ft/sec	$\frac{u_{(exp)}}{u_{(calc)}}$	$\frac{\Delta s}{\ell_L}$	$\frac{m_p A_L}{m_M A_p}$	T_F °K
140 (He)	20.5	13.0	45.05	3.50	21,000	200	11,800	0.681	0.117	1.33	5,100
141	20.5	13.0	44.15	3.00	22,000	200	12,200	0.826	0.097	1.51	3,500
142	20.5	9.1	60.00	3.00	20,000	200	14,400	0.830	0.194	2.06	5,140
143	20.5	9.1	44.19	3.00	20,000	200	14,500	0.910	0.193	1.52	4,660
144	20.5	9.1	87.60	1.80	24,000	200	17,000	0.681	0.279	5.02	7,240
145	20.5	9.1	87.64	1.75	24,000	200	16,100	0.653	0.289	5.16	7,020
146	20.5	9.1	87.06	1.30	26,000	100	18,400	0.504	0.208	6.90	14,300
147	20.5	9.1	87.18	1.50	26,000	150	18,000	0.586	0.261	5.99	10,300
148	20.5	8.54	87.22	1.50	23,000	150	18,100	0.627	0.280	5.99	9,400
149	20.5	9.31	87.55	1.50	23,000	150	18,500	0.634	0.254	6.02	9,400
150	20.5	8.57	87.57	1.50	25,000	150	17,400	0.593	0.270	6.02	9,660
151	10.5	9.38	87.72	1.50	20,000	250	19,300	0.799	0.147	6.13	5,970
160	10.5	9.60	87.50	1.00	23,000	225	23,500	0.810	0.167	9.02	7,170
169	10.5	9.83	86.53	2.00	16,000	250	18,350	0.950	0.071	4.46	4,410

Table 1 (Concluded)

Round	ℓ_p ft	ℓ_L ft	m_p g	m_M g	P_c psi	P_1 psia	$u_{(exp)}$ ft/sec	$\frac{u_{(exp)}}{u_{(calc)}}$	$\frac{\Delta s}{\ell_L}$	$\frac{m_p A_L}{m_M A_p}$	T_F °K
153 (H_2)	10.5	8.77	88.13	1.00	21,100	300	26,700	0.96	0.124	9.42	2,880
154	10.5	8.33	87.79	1.00	17,600	450	18,100	0.739	0.228	9.05	1,890
155	10.5	10.08	86.83	1.00	22,600	450	22,380	0.812	0.252	8.95	2,320
156	10.5	8.89	80.27	1.00	25,800	450	20,700	0.685	0.279	8.27	2,480
157	10.5	8.89	82.43	1.00	24,600	450	25,380	0.866	0.279	8.50	2,440
158	10.5	8.89	78.47	1.00	21,600	450	26,650	0.978	0.193	8.09	2,190
159	10.5	8.89	88.71	1.00	21,000	450	26,000	0.931	0.232	9.14	2,220

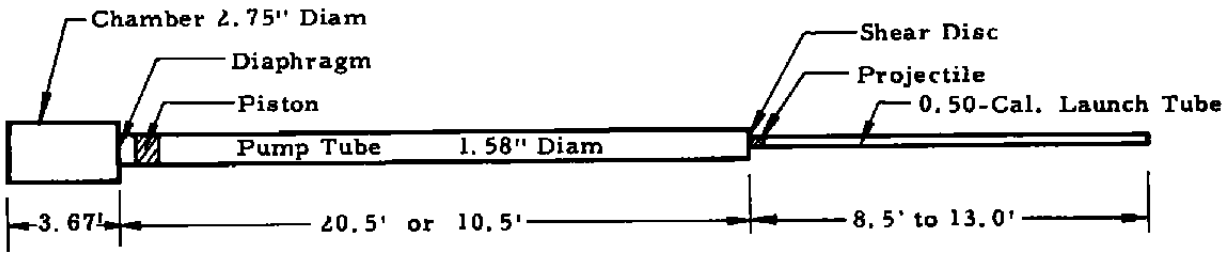

TABLE 2
AMES RESEARCH CENTER 20-MM LAUNCHER

(Ref. 1)

Round No.	P_c (psi)	P_1 (psi)	m_p (gm)	m_M (gm)	u_{exp} (ft/sec)	$\frac{u_{exp}}{u_{calc}}$	$\frac{m_p A_L}{m_M A_p}$	$\Delta s/\ell_L$	T_F °K
72	11,400	200	127	4.81	17,850	0.85	3.07	0.055	5,400
74	14,500	250	127	4.81	18,650	0.87	3.07	0.062	5,200
76s	17,300	250	127	4.81	18,800	0.82	3.07	0.061	5,800
79s	19,700	250	127	4.81	19,500	0.76	3.07	0.061	7,000
172s	9,200	300	127	4.81	15,300	0.85	3.07	0.078	3,800
72s	17,100	300	127	4.81	18,600	0.88	3.07	0.071	4,900
70	13,000	300	85	4.81	16,370	0.90	2.05	0.070	3,800
162s	20,000	300	127	6.43	18,000	0.86	1.89	0.058	5,300
57	15,100	300	127	8.60	17,380	0.97	1.71	0.059	4,500
131s	18,600	300	160	9.44	15,500	0.80	1.97	0.046	5,400
90	14,300	250	127	2.46	22,670	0.93	5.99	0.091	5,200
88	21,700	250	127	3.46	21,840	0.82	4.26	0.071	6,800
91	22,500	300	127	17.95	11,600	0.70	0.82	0.040	5,900

$(\ell/d)_L = 266$ $d_L = 0.766"$ $d_p = 2.25"$ $d_c = 4"$

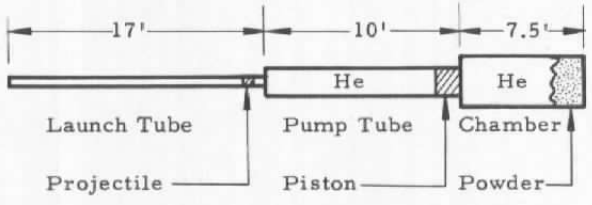

Note: Piston velocity calculated assuming H_2-O_2-He driver, 100-percent combustion

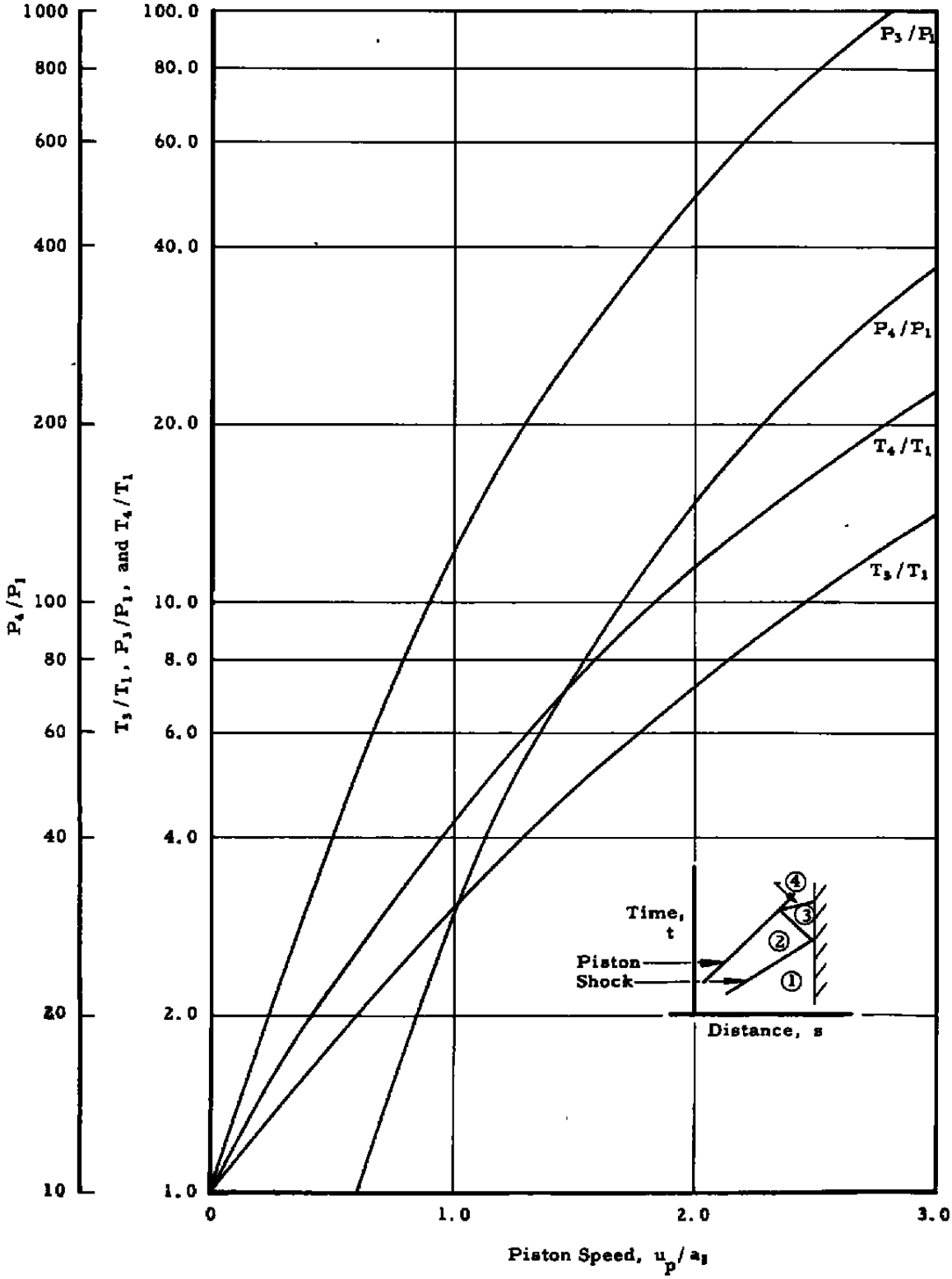

Fig. 1 Reflected Shock Conditions in Helium

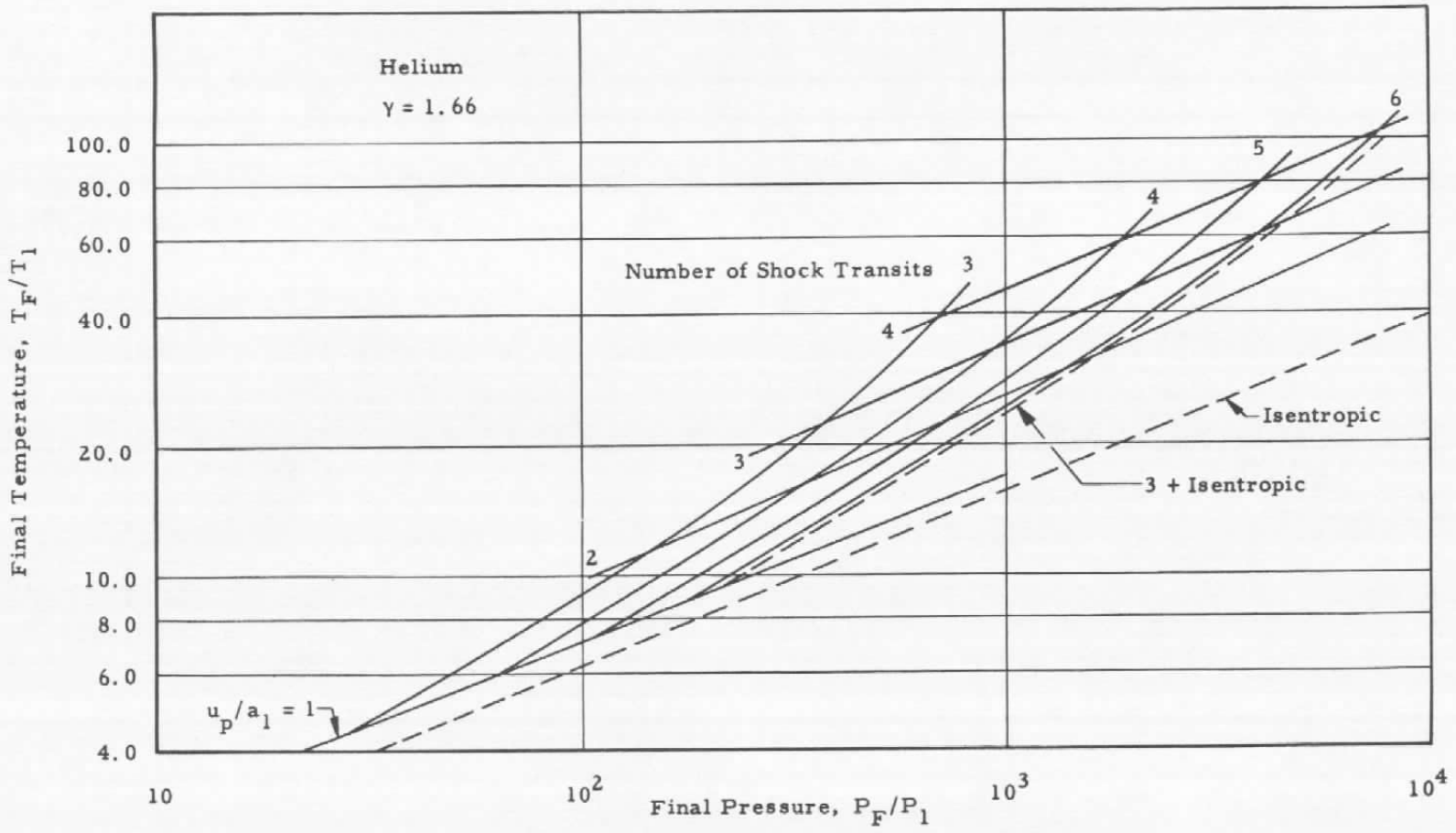

Fig. 2 Multiple Shock Compression

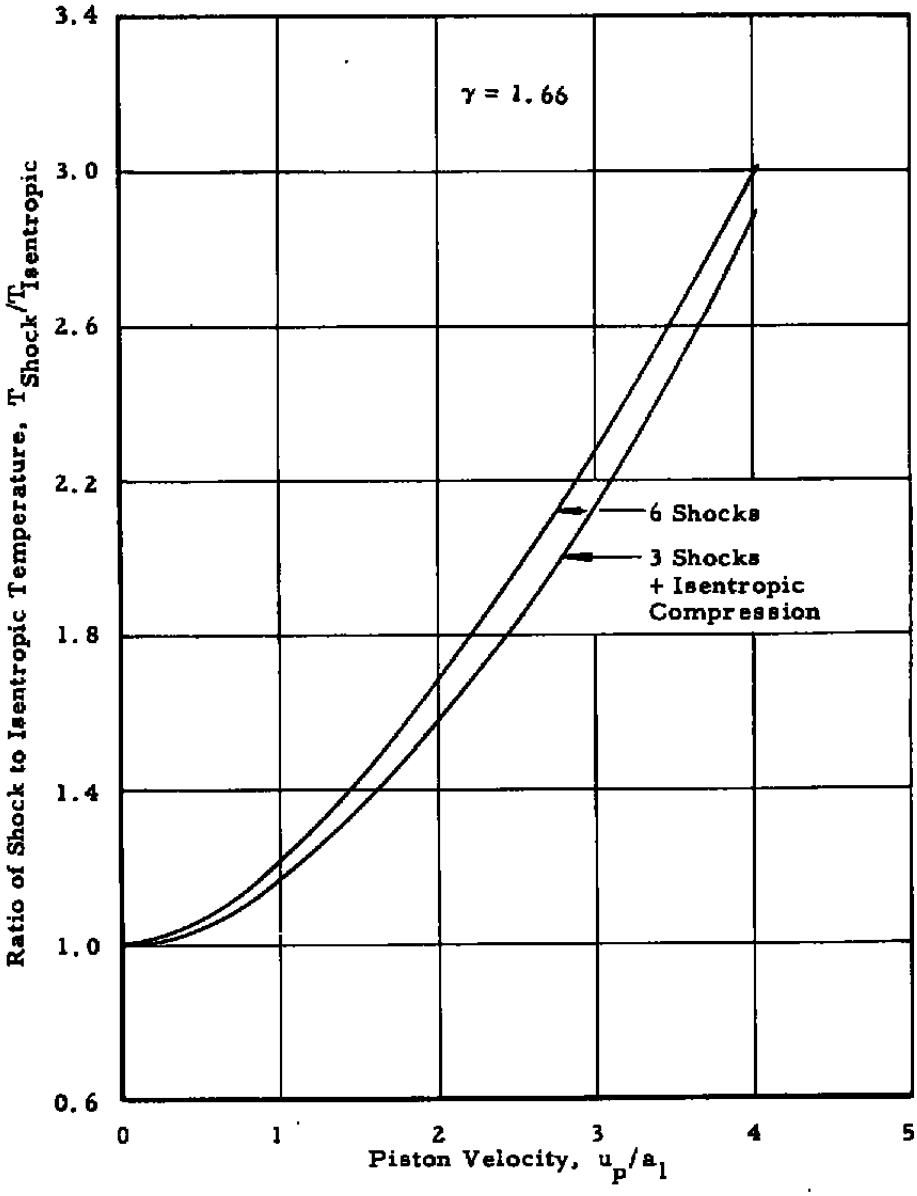

Fig. 3 Comparison of Shock and Isentropic Compression

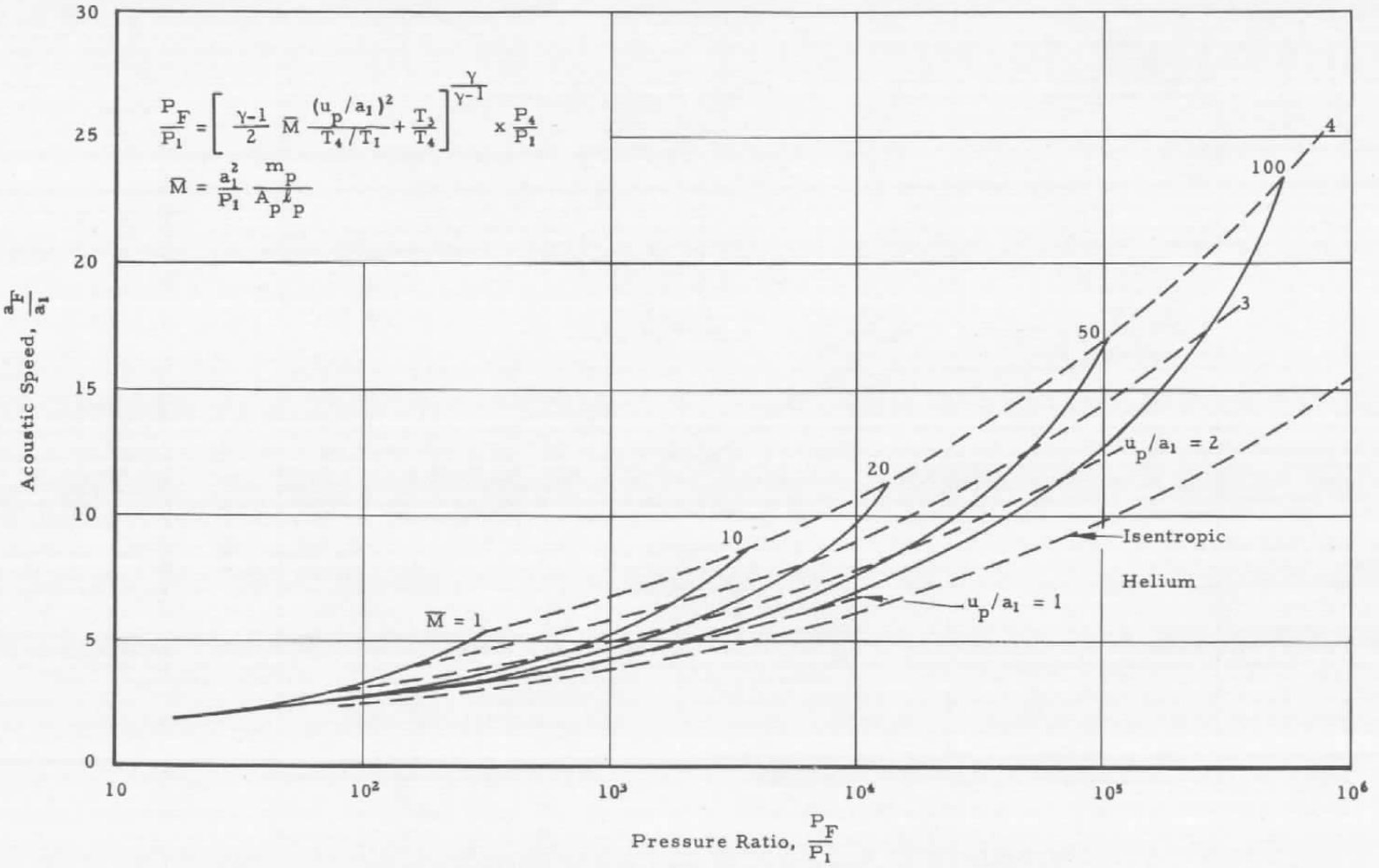

Fig. 4 General Pump Tube Characteristics

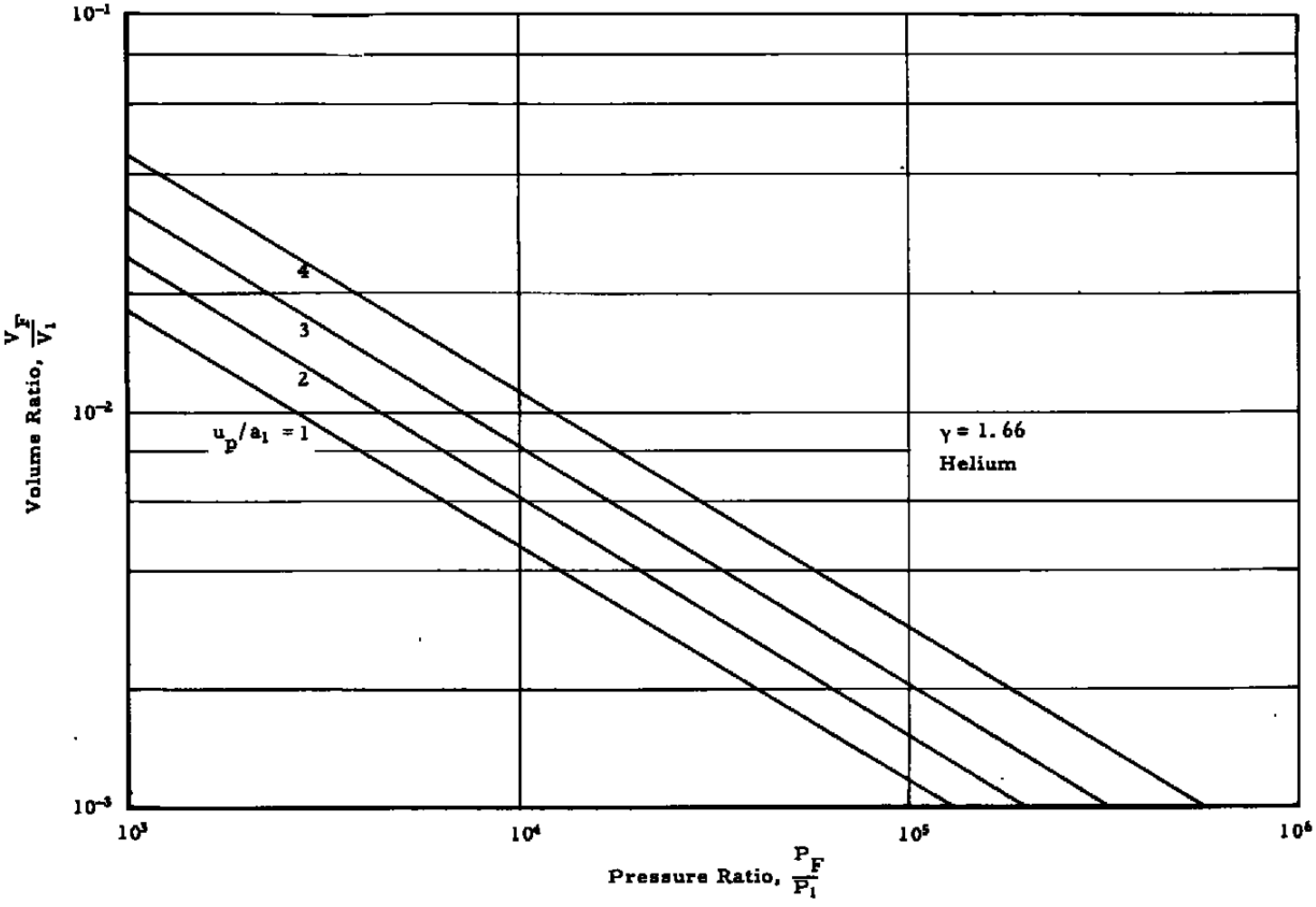

Fig. 4 Concluded

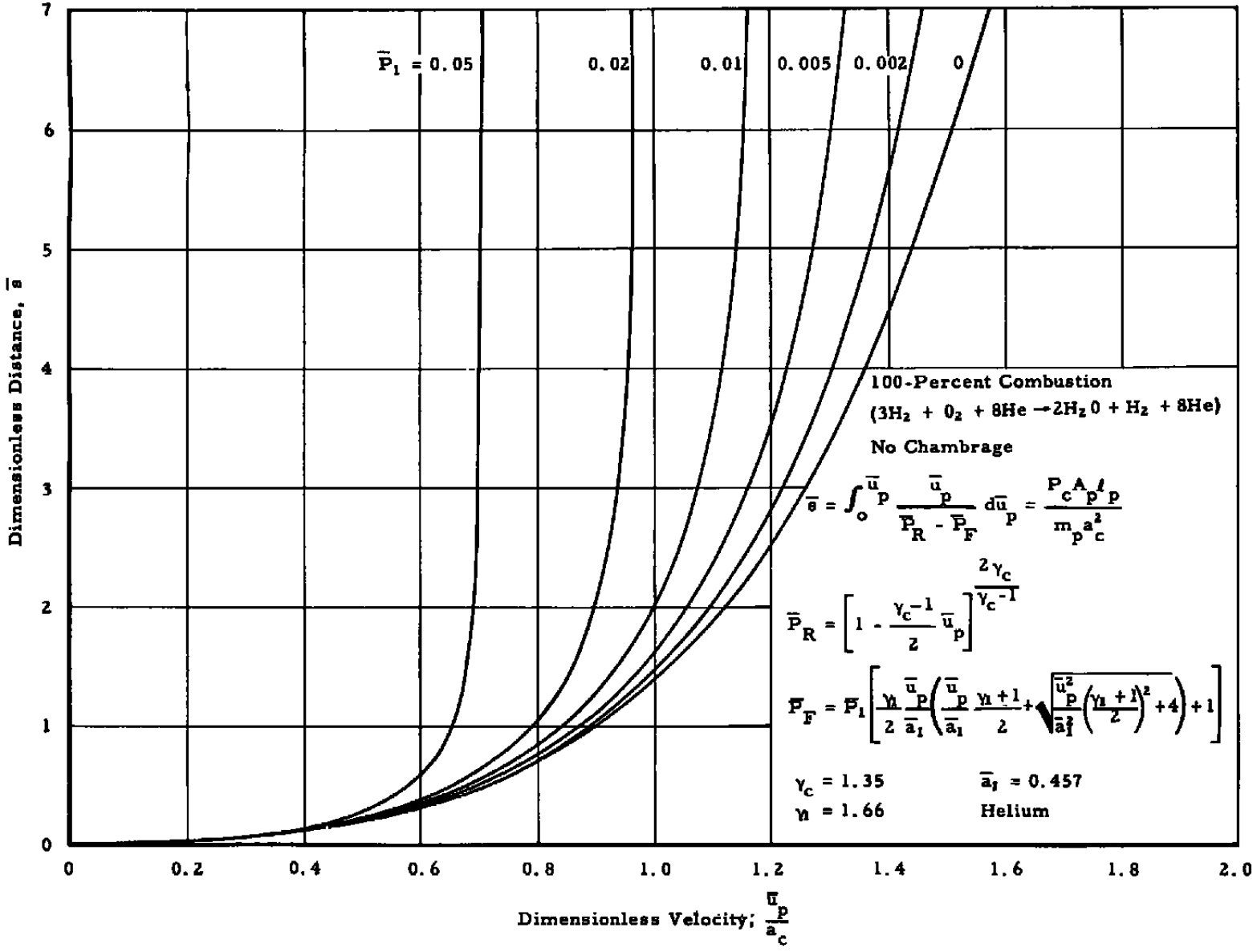

Fig. 5 Piston Speed – H_2- O_2 - He Combustion Driving Helium

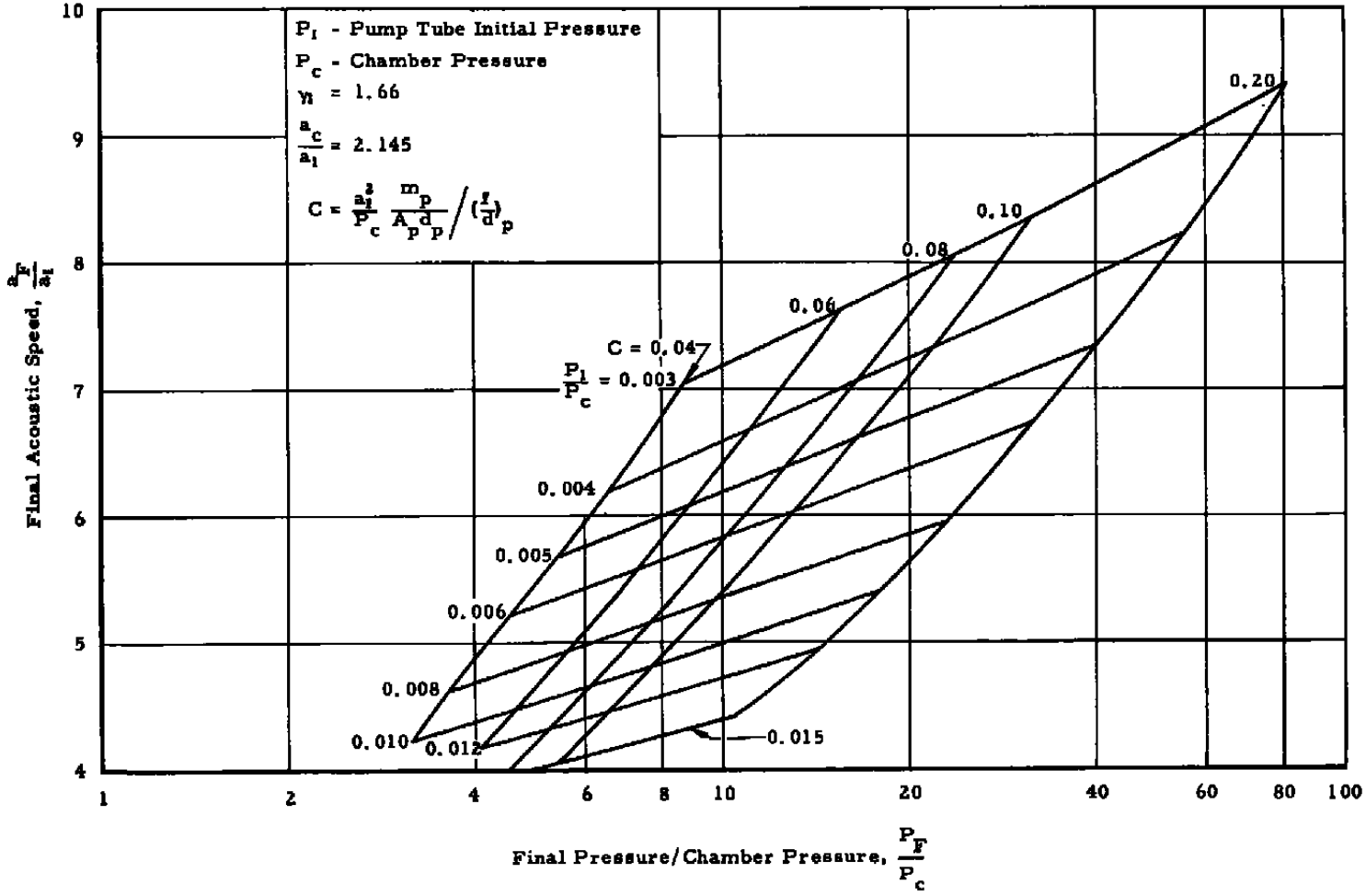

Fig. 6 General Pump Tube Characteristics Referred to Chamber Pressure (100-Percent Combustion)

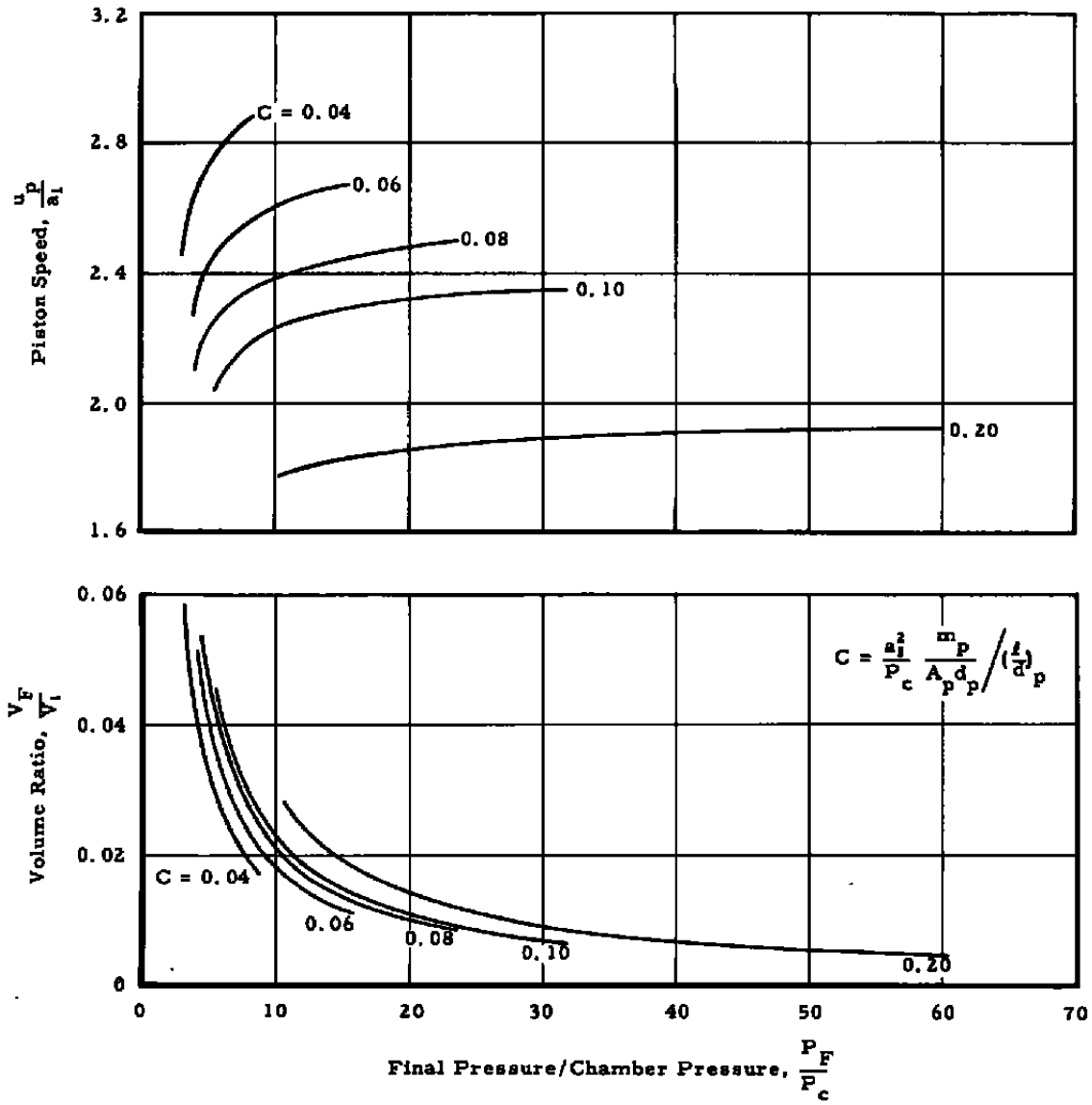

Fig. 6 Concluded

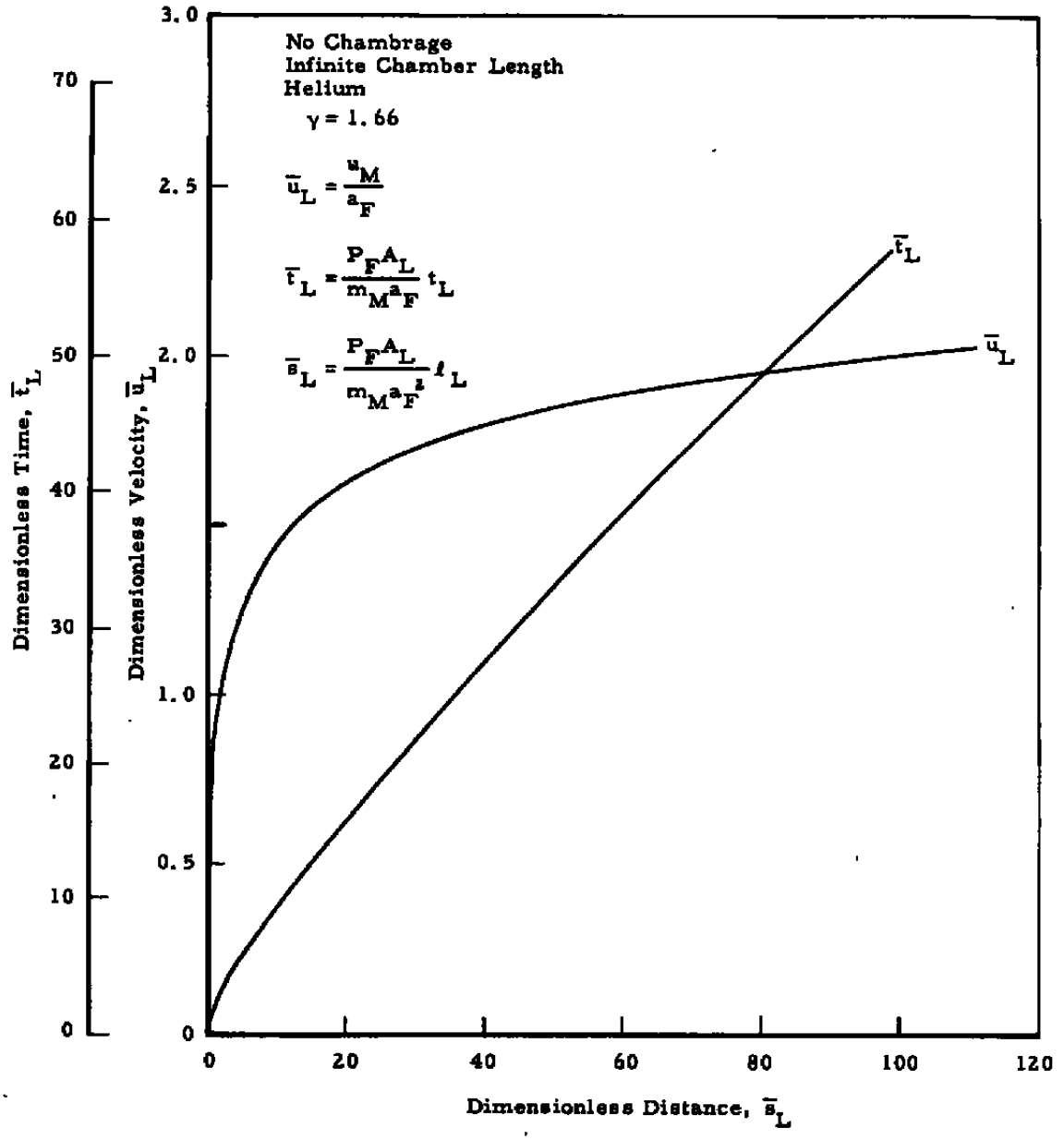

Fig. 7 Dimensionless Projectile Velocity and Time vs Dimensionless Distance

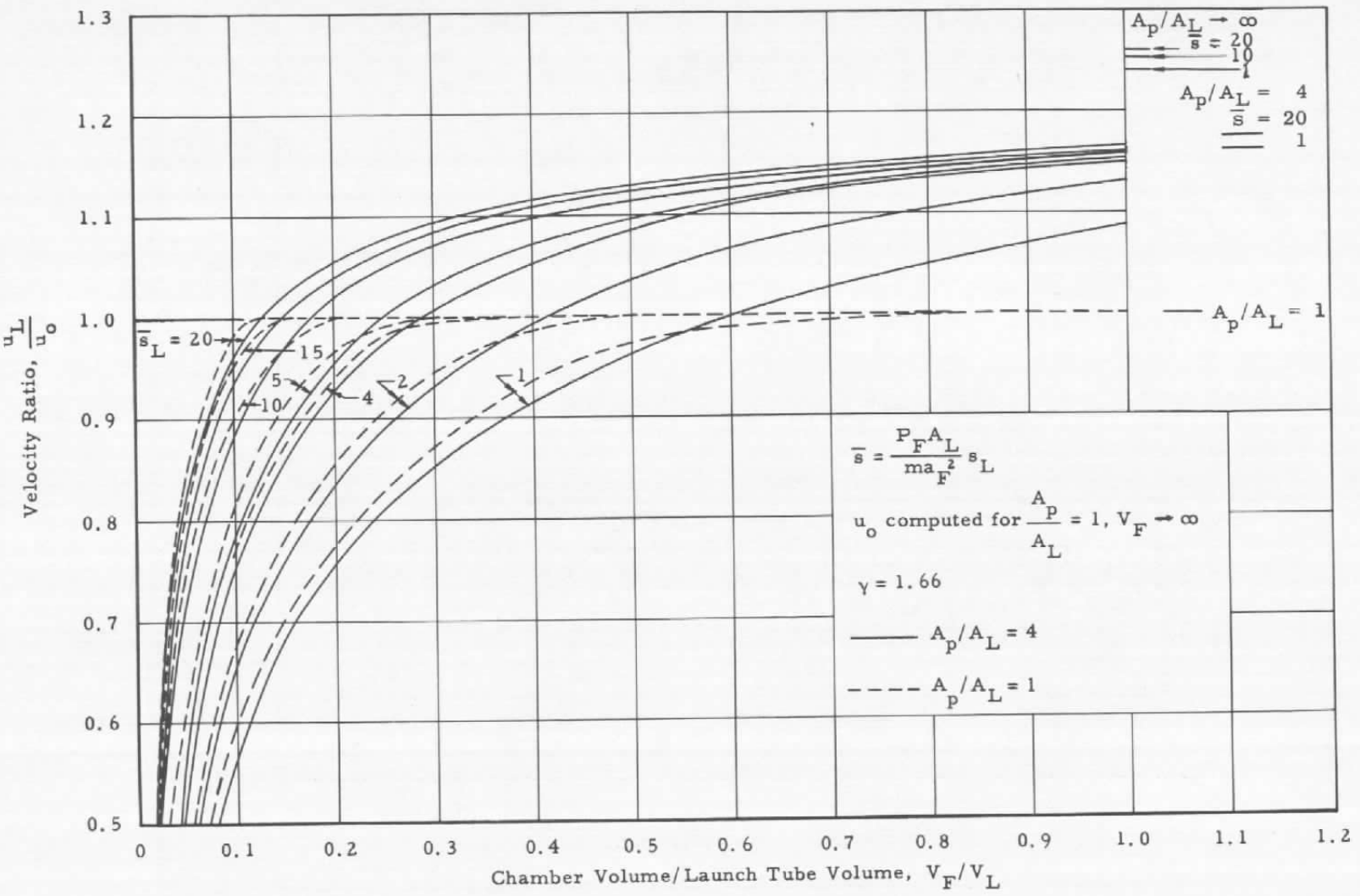

Fig. 8 Effect of Chamber Geometry on Launch Velocity

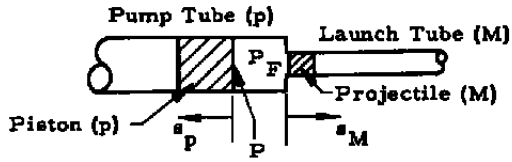

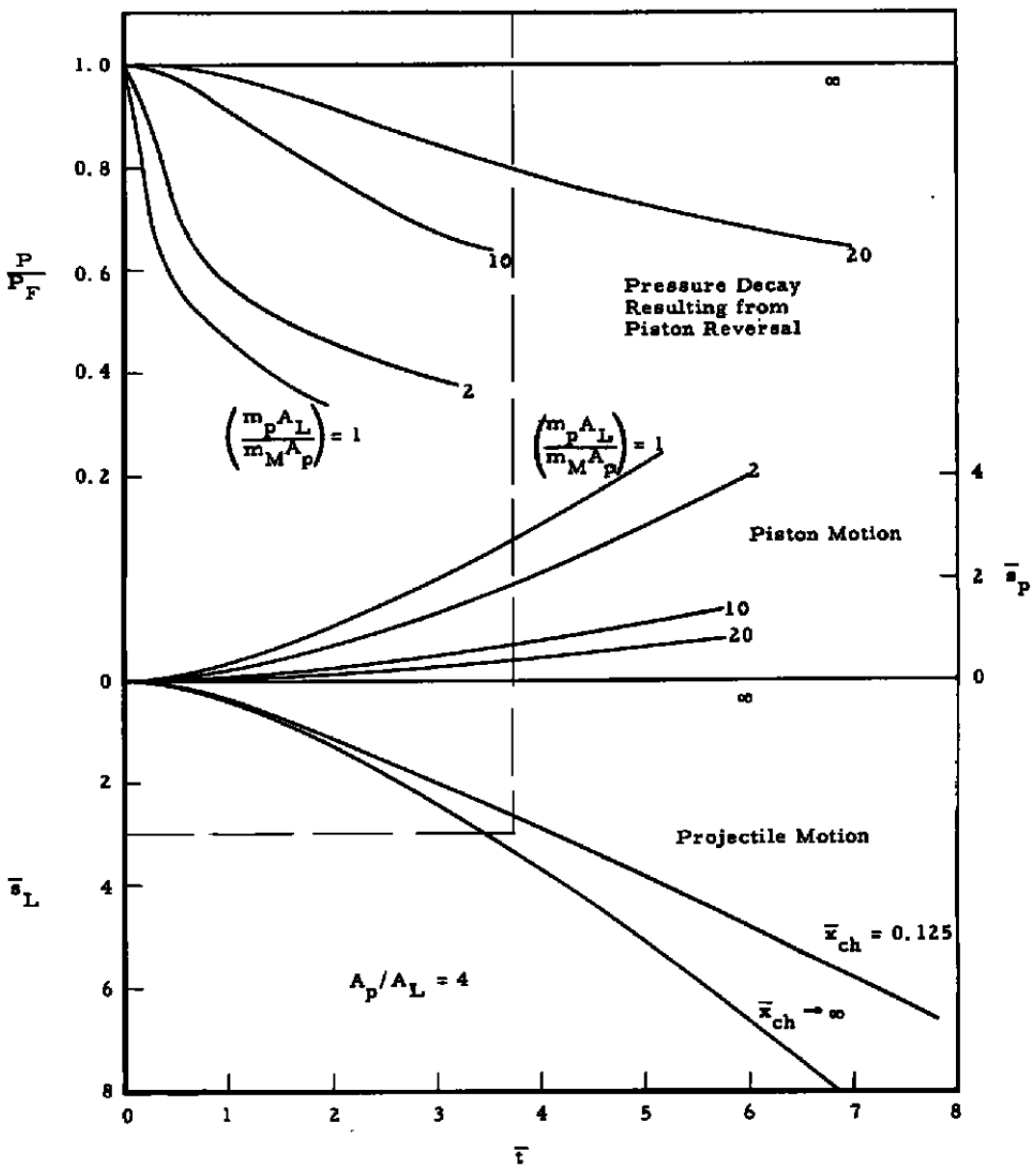

Fig. 9 Effect of Piston Mass Parameter

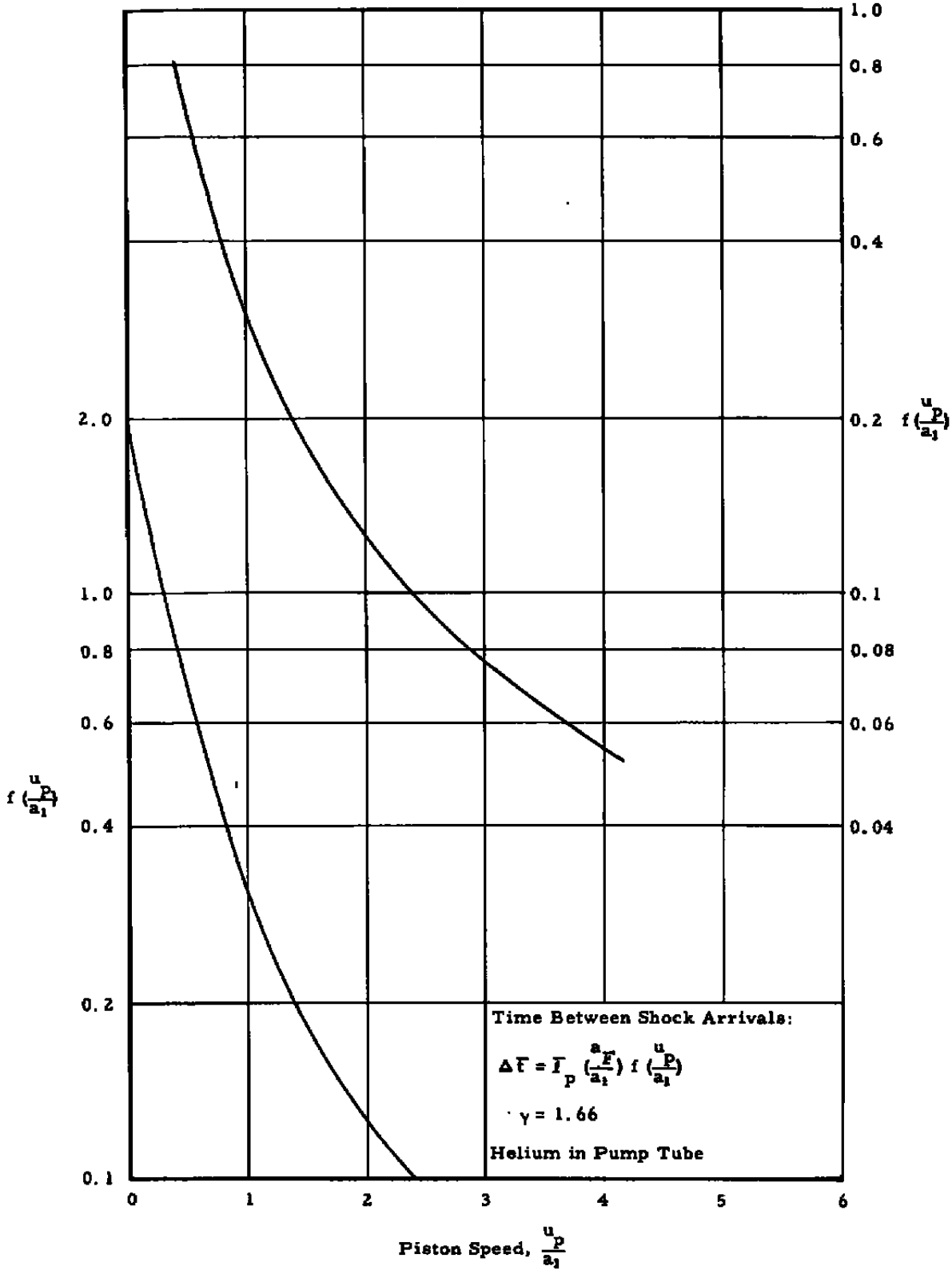

Fig. 10 Time Interval between First and Third Shock Reflections

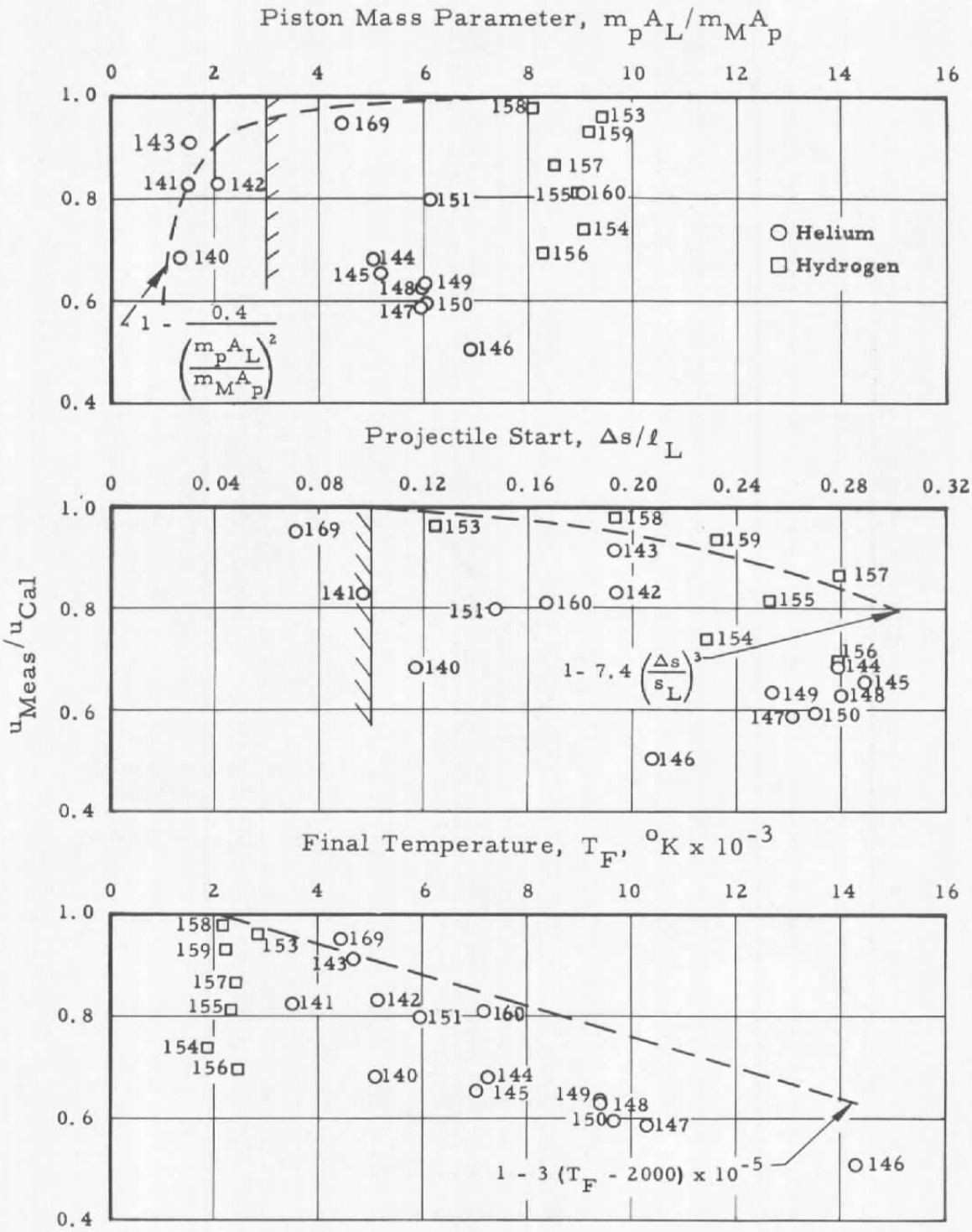

a. Effects of Piston Mass, Projectile Start, and Final Temperature

Fig. 11 Experimental Results for AEDC 2-Stage Launcher

Correlation Formula:

$$\frac{u}{u_{Cal}} = 1 - \frac{0.4}{\left(\frac{m_p A_L}{m_M A_p}\right)^2} - 7.4\left(\frac{\Delta s}{s_L}\right)^3 - 3\,(T_F - 2000) \times 10^{-5}$$

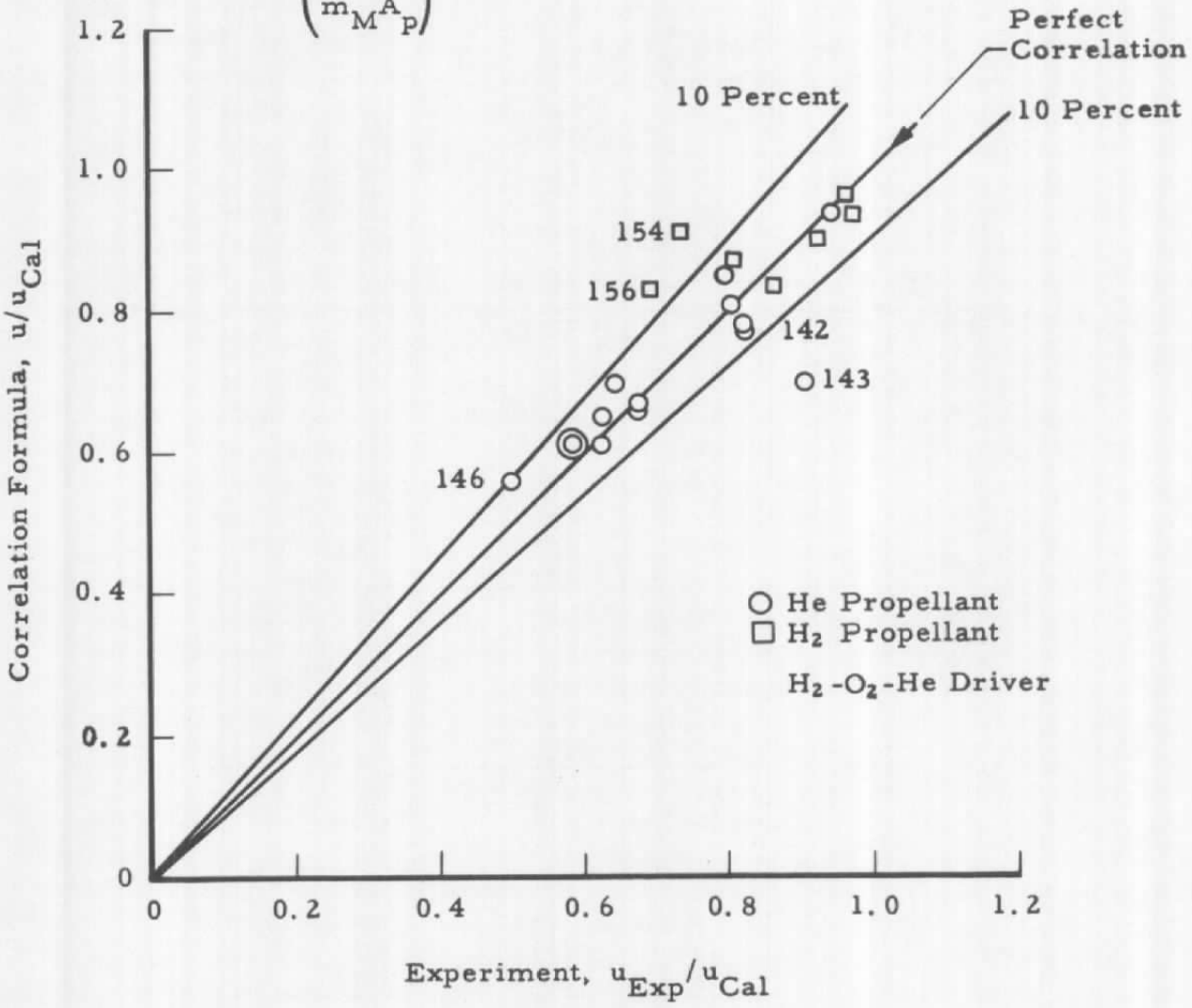

b. Empirical Correlation

Fig. 11 Concluded

Correlation Formula From AEDC Data:

$$\frac{u}{u_{Cal}} = 1 - \frac{0.4}{\left(\frac{m_p A_L}{m_M A_p}\right)^2} - 7.4\left(\frac{\Delta s}{s_L}\right)^3 - 3\,(T_F - 2000) \times 10^{-5}$$

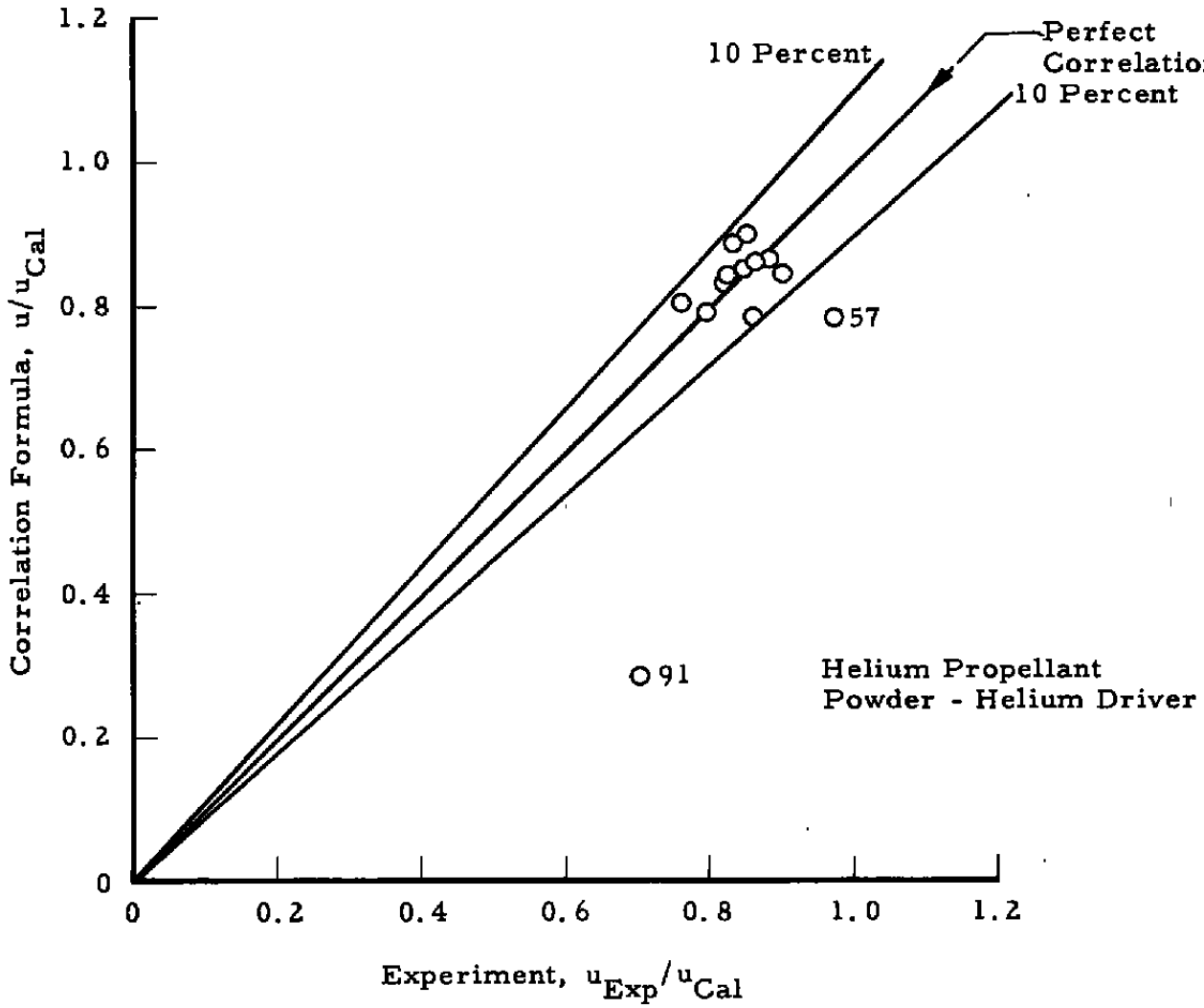

Fig. 12 Correlation of Experimental Results for Ames Research Center Launcher

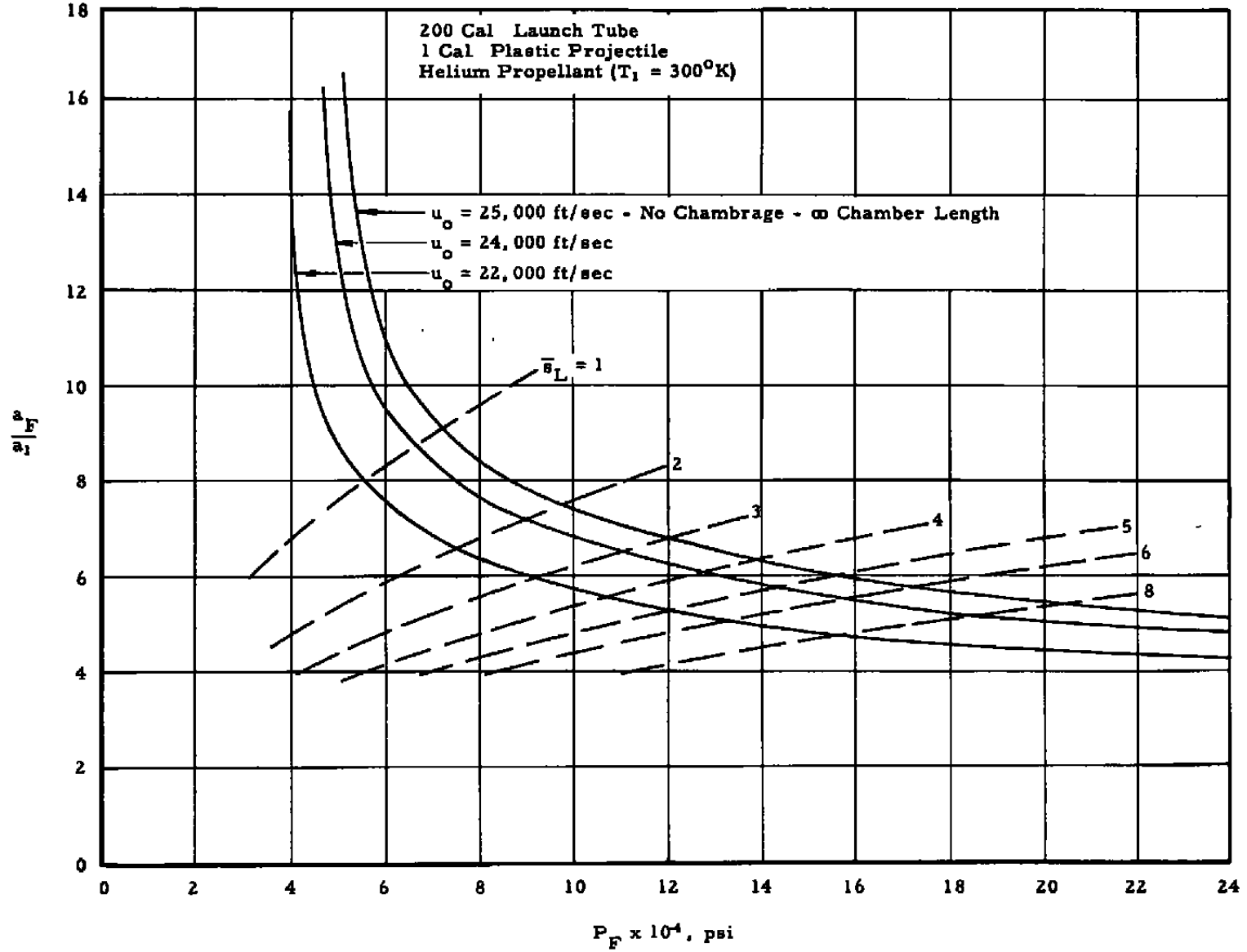

Fig. 13 Launch Tube Requirements

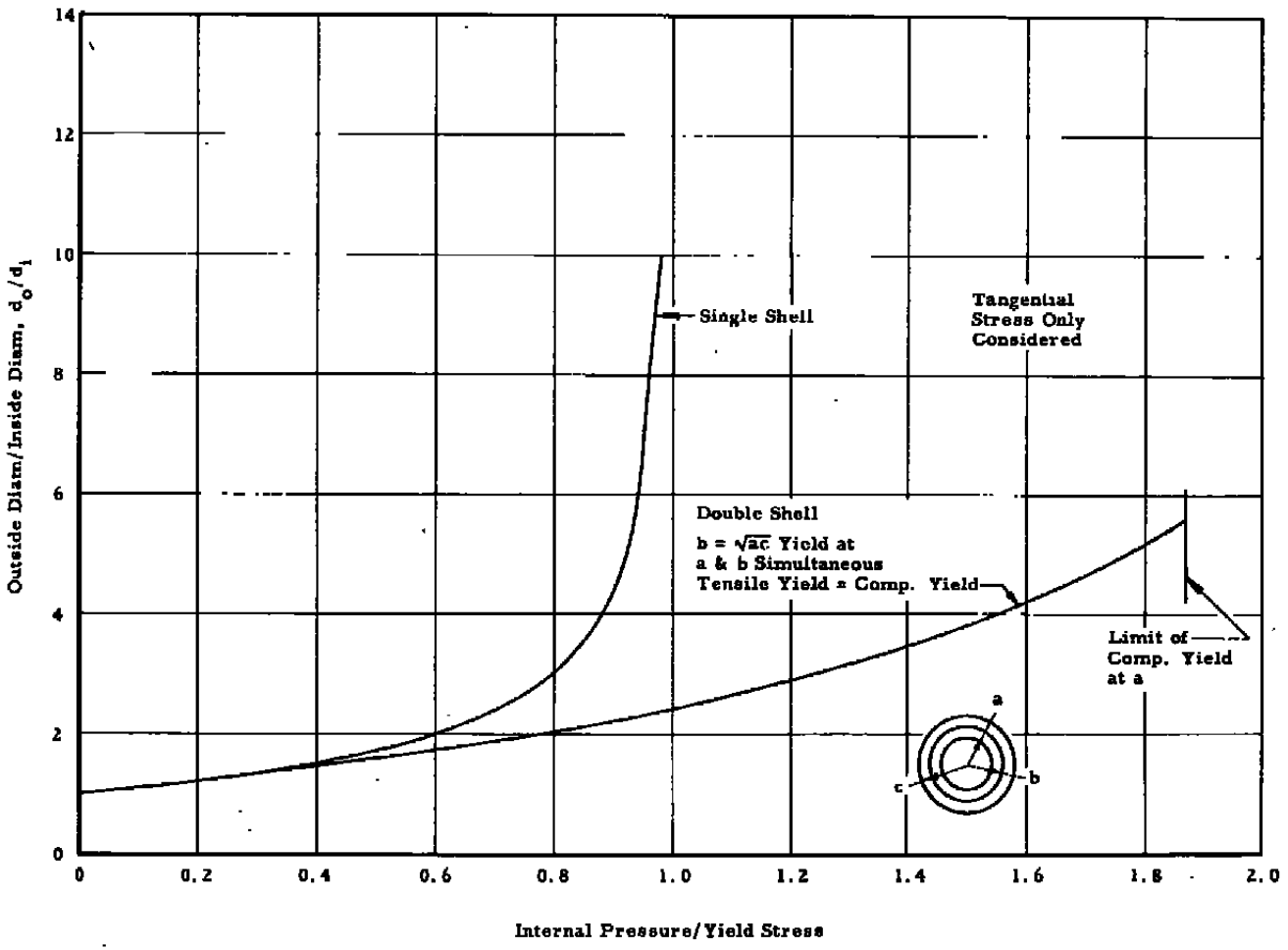

Fig. 14 Diameter Ratio vs Internal Pressure for Cylindrical Vessels

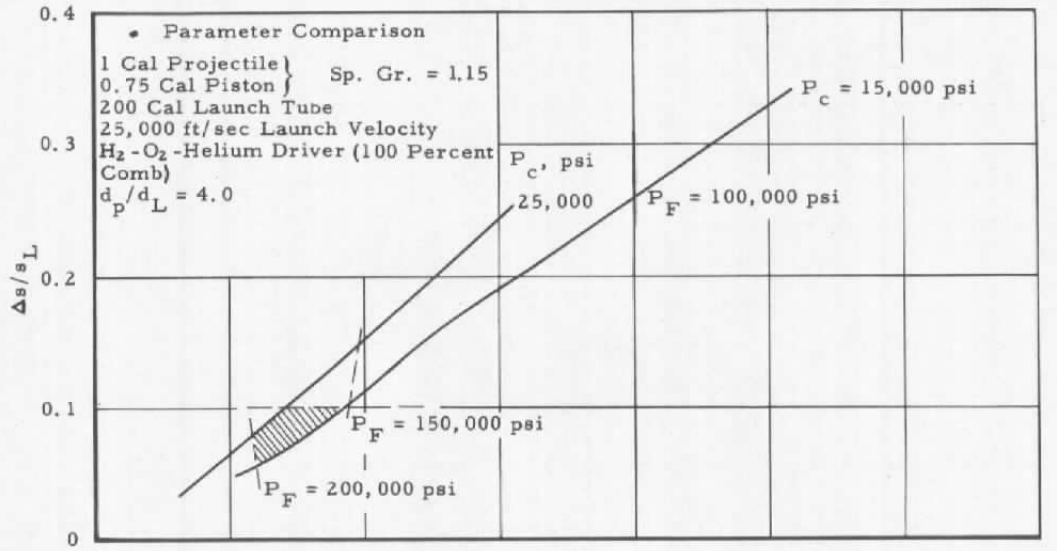

a. Initial Projectile Motion

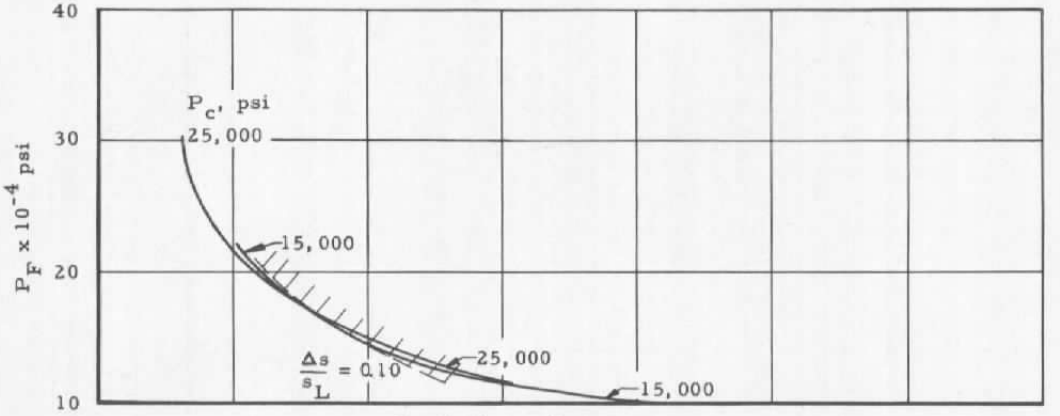

b. Maximum Pressure

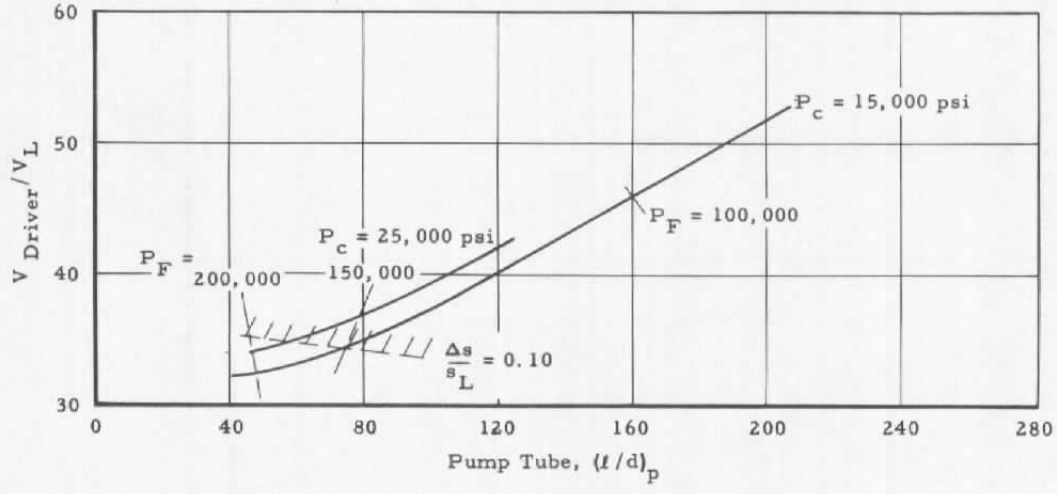

c. Driver Volume

Fig. 15 Launcher Characteristics – Minimum Weight Piston (0.75-caliber Plastic)

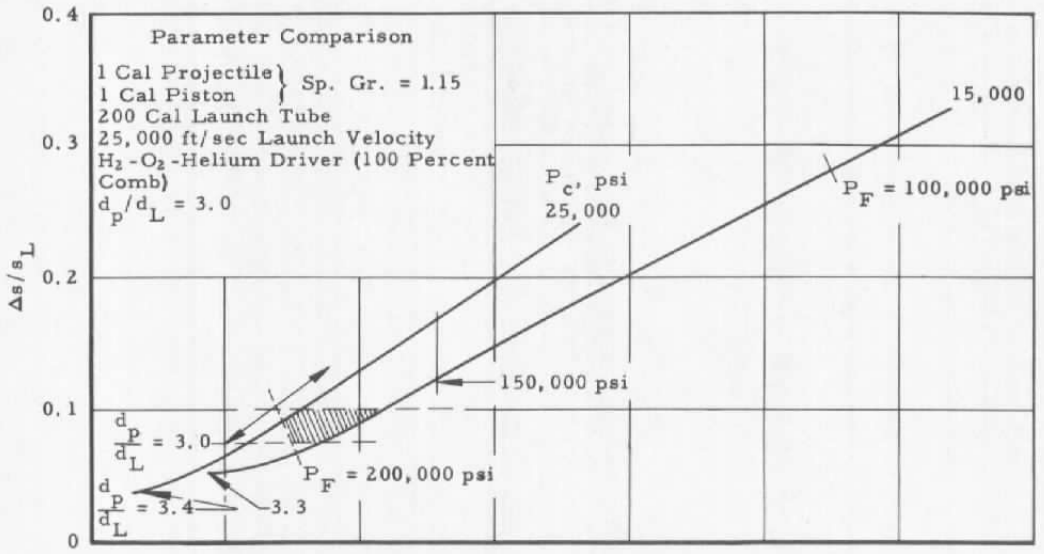

a. Initial Projectile Motion

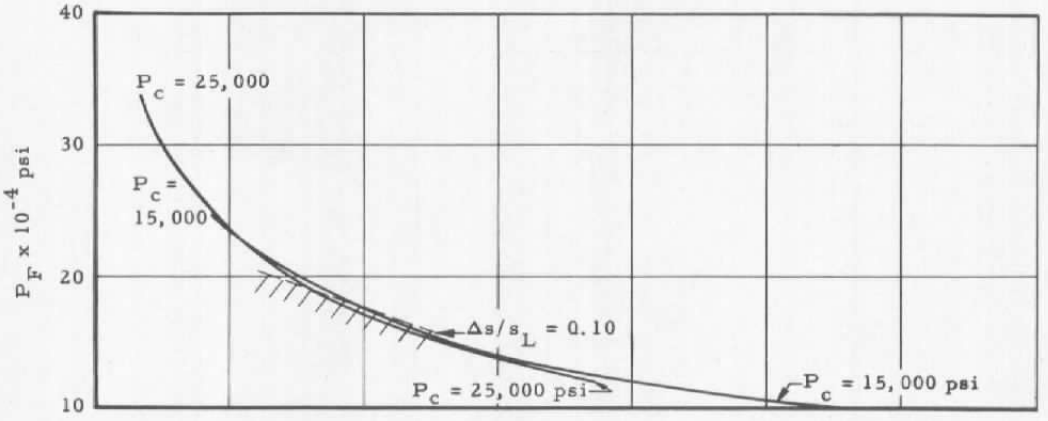

b. Maximum Pressure

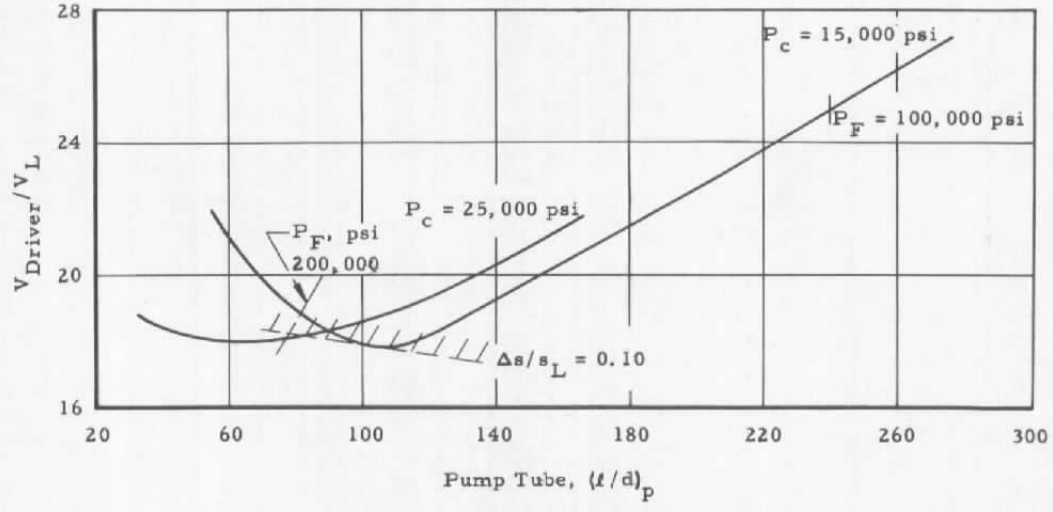

c. Driver Volume

Fig. 16 Launcher Characteristics – 1-Caliber Length Plastic Piston

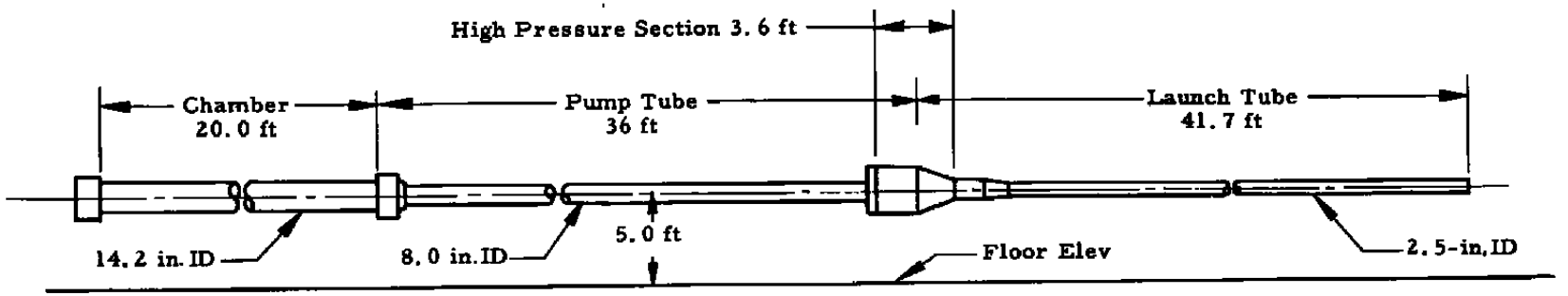

Fig. 17 Configuration of 2.5-Inch Launcher

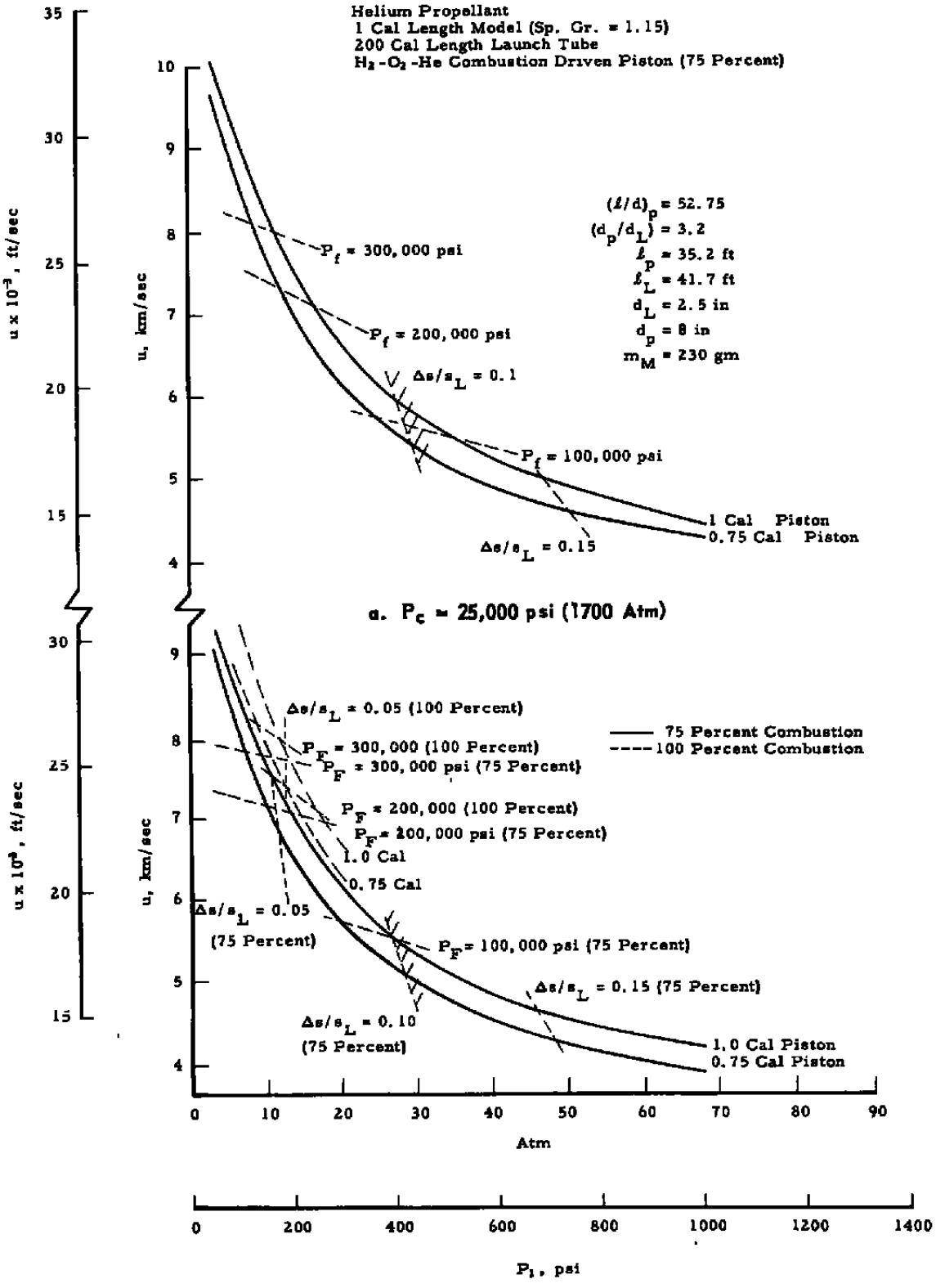

Fig. 18 Estimated Performance of Launcher